A Kinetic, Mechanistic, and Molecular Mechanics Investigation of Olefin Insertion into Organoactinide-Hydride Bonds. Metal, Olefin, Ancillary Ligand, and Diastereoselection Effects

Zerong Lin and Tobin J. Marks*

Contribution from the Department of Chemistry, Northwestern University, Evanston, Illinois 60208. *Received September 21, 1989*

Abstract: This contribution reports a kinetic/mechanistic/stereochemical/molecular mechanics study of olefin insertion into the actinide-hydrogen bonds of $Cp'_2An(H)(OR)$ complexes ($Cp' = \eta^5$-$(CH_3)_5C_5$; An = Th, U; R = achiral or chiral alkyl group). For the reaction $Cp'_2An(H)(O$-t-$Bu)$ + cyclohexene (An = Th), the rate law is first order in organoactinide and first order in olefin, with $k_{Th-H}/k_{Th-D} = 1.4$ (1), $k_{THF}/k_{toluene} = 0.59$ (5), $\Delta H^{\ddagger} = 9.0$ (5) kcal/mol, and $\Delta S^{\ddagger} = -47.2$ (1) eu; $k_U/k_{Th} \approx 1.5$. For $Cp'_2Th(H)[OCH(t\text{-}Bu)_2]$ + 1-hexene, $k_{Th-H}/k_{Th-D} = 1.3$ (2). Alkoxide effects on insertion rates can be large, and for $Cp'_2Th(H)(OR)$ + cyclohexene, $k_{O\text{-}t\text{-}Bu}/k_{OCH(t\text{-}Bu)_2} \gtrsim 10^3$. For $Cp'_2Th(H)[OCH(t\text{-}Bu)_2]$, relative insertion rates follow the ordering ethylene > 1-hexene > 4-methoxystyrene > styrene ≫ cyclohexene; $k_{4\text{-methoxystyrene}}/k_{styrene} = 2.2$ (5). For *cis*-2-butene, insertion reactions yield *sec*-butyl derivatives that slowly rearrange to the *n*-butyl isomers. Insertion experiments with $Cp_2'An(H)(OR^*)$ complexes having chiral alkoxide ligands (OR^* = (1*R*,2*S*,5*R*)-menthoxide; (*R*)-2-butoxide; [(1*S*)-*endo*]-bornoxide; (1*S*,2*S*,5*R*)-neomenthoxide) and prochiral olefins (norbornene, *cis*-2-butene) or ketones (acetophenone, butyrophenone) demonstrate that maximum diastereoselection occurs for sterically encumbered reagents at low temperatures (de = 36% for norbornene at −45 °C). A molecular mechanics/molecular graphics analysis suggests that the sterically most favorable direction of olefin approach toward the actinide center is between the U-H and U-O bonds rather than from the side. These results provide additional insight into ancillary ligand effects on the kinetics of organo-f-element-catalyzed olefin hydrogenation.

The insertion of olefinic functionalities into metal-hydride bonds is a crucial step in numerous stoichiometric, homogeneous catalytic, and heterogeneous catalytic processes occurring at d^0 transition element and f element centers.[1-5] Mechanistically, such insertion processes are not in general well-understood and are necessarily operative in very different metal-ligand environments than the more extensively studied analogues at middle- and late-transition element centers.[6,7] Thus, the d^0/f metal ion is likely

Scheme I

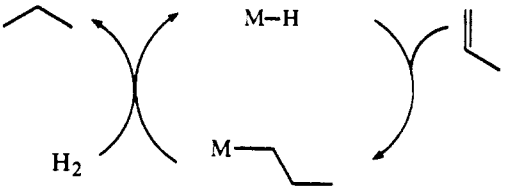

to be in a relatively high formal oxidation state, to be electronically incapable of extensive π back-bonding or stable olefin complex formation, to be engaged in relatively polar metal-ligand bonding with a strong affinity for "hard" ligands, and to exhibit unusual M-C(hydrocarbyl)/M-H bond disruption enthalpy patterns vis-ă-vis those of later transition metals.[8,9] In this laboratory, interest in such transformations derives primarily from studies of organolanthanide[10]/organoactinide[4c,5,11] olefin hydrogenation

(1) (a) Cardin, D. J.; Lappert, M. F.; Raston, C. L. *Chemistry of Organo-Zirconium and -Hafnium Compounds*; Ellis Horwood Ltd.: New York, 1986; Chapters 6, 12, and 20. (b) Roddick, D. M.; Fryzuk, M. D.; Seidler, P. F.; Hillhouse, G. L.; Bercaw, J. E. *Organometallics* **1985**, *4*, 97-100, and references therein. (c) Schwartz, J.; Labinger, J. A. In *New Synthetic Methods*; Verlag Chemie: New York, 1979; Vol. 5. (d) Schwartz, J.; Labinger, J. A. *Angew. Chem., Int. Ed. Engl.* **1976**, *6*, 333-340.

(2) (a) Keii, T., Soga, K., Eds. *Catalytic Polymerization of Olefins*; Elsevier: Amsterdam, 1986. (b) Firment, L. E. *J. Catal.* **1983**, *82*, 106-212, and references therein. (c) Yermakov, Y. I. *J. Mol. Catal.* **1983**, *21*, 35-55, and references therein. (d) Kuznetsov, B. N.; Zakharov, V. A. *Catalysis by Supported Complexes*; Elsevier: Amsterdam, 1981.

(3) (a) Schumann, H. In *Fundamental and Technological Aspects of Orgao-f-Element Chemistry*; Marks, T. J., Fragală, I., Eds.; D. Reidel: Dordrecht, Holland, 1985; Chapter 1. (b) Evans, W. J. *Adv. Organomet. Chem.* **1985**, *24*, 131-177. (c) Watson, P. L.; Parshall, G. W. *Acc. Chem. Res.* **1985**, *18*, 51-56.

(4) (a) Marks, T. J. In *The Chemistry of the Actinide Elements*, 2nd ed.; Katz, J. J., Seaborg, G. T., Morss, L. R., Eds.; Chapman and Hall: London, 1986; Chapter 23. (b) Marks, T. J.; Day, V. W. In *Fundamental and Technological Aspects of Organo-f-Element Chemistry*; Marks, T. J., Fragală, I. L., Eds. Reidel: Dordrecht, 1985; Chapter 4. (c) Fagan, P. J.; Manriquez, J. M.; Maatta, E. A.; Seyam, A. M.; Marks, T. J. *J. Am. Chem. Soc.* **1981**, *103*, 6650-6667.

(5) (a) Gillespie, R. D.; Burwell, R. L., Jr.; Marks, T. J. *Langmuir*, in press. (b) Burwell, R. L., Jr.; Marks, T. J. In *Catalysis of Organic Reactions*; Augustine, R. L., Ed.; Marcel Dekker, Inc.: New York, 1985; pp 207-224. (c) He, M.-Y.; Xiong, G.; Toscano, P. J.; Burwell, R. L., Jr.; Marks, T. J. *J. Am. Chem. Soc.* **1985**, *107*, 641-652. (d) He, M.-Y.; Burwell, R. L., Jr.; Marks, T. J. *Organometallics* **1983**, *2*, 566-569.

(6) (a) Collman, J. P.; Hegedus, L. S.; Norton, J. R.; Finke, R. G. *Principles and Applications of Organotransition Metal Chemistry*; University Science: Mill Valley, CA, 1987; Chapters 6.3, 10, 13. (b) James, B. R. In *Comprehensive Organometallic Chemistry*; Wilkinson, G., Stone, F. G. A., Abel, E. W., Eds. Pergamon Press: Oxford, 1982; Chapter 51. (c) Masters, C. *Homogeneous Transition-metal Catalysis*; Chapman and Hall: London, 1981; Chapter 2.1. (d) Parshall, G. W. *Homogeneous Catalysis*; Wiley-Interscience: New York, 1980; Chapter 3.

(7) (a) Burger, B. J.; Santarsiero, B. D.; Trimmer, M. S.; Bercaw, J. E. *J. Am. Chem. Soc.* **1988**, *110*, 3134-3146, and references therein. (b) Doherty, N. M.; Bercaw, J. E. *J. Am. Chem. Soc.* **1985**, *107*, 2670-2682, and references therein. (c) Halpern, J.; Okamoto, T. *Inorg. Chim. Acta* **1984**, *89*, L53-L54. (d) Roe, D. C. *J. Am. Chem. Soc.* **1983**, *105*, 7770-7771. (e) Halpern, J.; Okamoto, T.; Zakhariev, A. *J. Mol. Catal.* **1976**, *2*, 65-68. (f) Byne, J. W.; Blaser, H. U.; Osborn, J. A. *J. Am. Chem. Soc.* **1975**, *97*, 3871-3873.

(8) (a) Schock, L. E.; Marks, T. J. *J. Am. Chem. Soc.* **1988**, *110*, 7701-7715. (b) Bulls, A. R.; Bercaw, J. E.; Manriquez, J. M.; Thompson, M. E. In Metal-Ligand Bonding Energetics in Organotransition Metal Compounds. *Polyhedron Symposium-in-Print*; Marks, T. J., Ed.; **1988**, *7*, 1409-1428.

(9) (a) Nolan, S. P.; Stern, D.; Marks, T. J. *J. Am. Chem. Soc.* **1989**, *111*, 7844-7853. (b) Schock, L. E.; Seyam, A. M.; Marks, T. J., in ref 8b, pp 1517-1530. (c) Bruno, J. W.; Stecher, H. A.; Morss, L. R.; Sonnenberger, D. C.; Marks, T. J. *J. Am. Chem. Soc.* **1986**, *108*, 7275-7280. (d) Sonnenberger, D. C.; Morss, L. R.; Marks, T. J. *Organometallics* **1985**, *4*, 352-355. (e) Bruno, J. W.; Marks, T. J.; Morss, L. R. *J. Am. Chem. Soc.* **1983**, *105*, 6824-6832.

(10) (a) Mauermann, H.; Swepston, P. N.; Marks, T. J. *Organometallics* **1985**, *4*, 200-202. (b) Jeske, G.; Lauke, H.; Mauermann, H.; Swepston, P. N.; Schumann, H.; Marks, T. J. *J. Am. Chem. Soc.* **1985**, *107*, 8091-8103. (c) Jeske, G.; Schock, L. E.; Swepston, P. J.; Schumann, H.; Marks, T. J. *J. Am. Chem. Soc.* **1985**, *107*, 8103-8110. (d) Jeske, G.; Lauke, H.; Mauermann, H.; Schumann, H.; Marks, T. J. *J. Am. Chem. Soc.* **1985**, *107*, 8111-8118.

0002-7863/90/1512-5515$02.50/0

catalysis, where such insertion processes constitute one leg of the proposed catalytic cycle (e.g., Scheme I). We recently reported a detailed mechanistic investigation of the hydrogenolytic component of this cycle and probed metal, alkyl group, and ancillary ligand effects for a series of $Cp'_2An(X)R$ complexes (An = Th, U; $Cp' = \eta^5$-$(CH_3)_5C_5$).[12] We now present a complementary mechanistic study of the alkene insertion process (eq 1), focusing

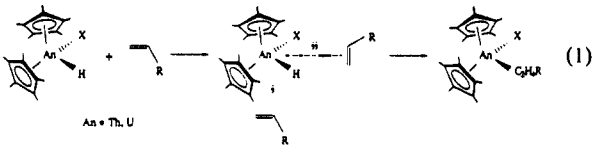

(1)

in a manner correlated with the first study, upon metal, alkene, and ancillary ligand (X) effects on this transformation. The surprisingly large X ligand kinetic effects observed have in addition prompted a computational/molecular mechanics/molecular graphics analysis of steric interactions along the plausible reaction coordinates (e.g., trajectory i vs ii in eq 1), as well as an experimental investigation of diastereoselection in cases of chiral X ligands and prochiral substrates. The latter study accompanies the observation of large asymmetric induction effects for olefin activation by certain chiral organolanthanides[13] and the facility of NMR-based stereochemical analyses in paramagnetic U(IV) systems. In the process, we also report the synthesis and characterization of several new classes of chiral organoactinides.

Experimental Section

Materials and Methods. All organoactinide compounds investigated are exceedingly air- and moisture-sensitive and, hence, were handled in Schlenk-type glassware interfaced to a high vacuum line, or on a Schlenk line, or in an N_2-filled glovebox. Solvents were predried and distilled from Na/K/benzophenone.[14a] The gases Ar, H_2, and N_2 were purified by passage through a supported MnO oxygen removal column and a Davison 4-Å molecular sieve column. D_2, CO_2, ethylene, 1-butene, and *cis*-2-butene were purified by passage through a supported MnO trap.

The actinide complexes Cp'_2ThCl_2,[4c] Cp'_2UCl_2,[4c] $Cp'_2U(CH_2TMS)_2$,[4c] $Cp'_2Th(H)(O\text{-}t\text{-}Bu)$ (**1H**),[14b] $Cp'_2Th(D)(O\text{-}t\text{-}Bu)$ (**1D**),[14b] $Cp'_2Th(H)[OCH(t\text{-}Bu)_2]$ (**2H**),[15] $Cp'_2Th(D)[OCH(t\text{-}Bu)_2]$ (**2D**),[15] and $Cp'_2U(CH_2\text{-}t\text{-}Bu)(O\text{-}t\text{-}Bu)$,[12] as well as the reagents $LiCH_2TMS$,[16] α-ethylstyrene,[17] and 2-ethyl-1-hexene[18] were prepared according to the literature procedures. The olefins and ketones 1-hexene (Aldrich), styrene (Aldrich), 4-vinylanisole (Aldrich), acetophenone (Aldrich), and butyrophenone (Aldrich) were freeze–pump–thaw degassed three times and dried over freshly activated 4-Å molecular sieves for several days before use. Cyclohexene (Aldrich) was dried over Na/K for several days prior to use. Sodium lumps (Mallinckrodt, in mineral oil) were washed with dry pentane immediately before use. Norbornene was sublimed under high vacuum and stored in an anaerobic storage tube. The chiral alcohols (1*R*,2*S*,5*R*)-(−)-menthol, (*R*)-(−)-2-butanol, [(1*S*)-*endo*]-(−)-borneol, and (1*S*,2*S*,5*R*)-(+)-neomenthol were commercially available (Aldrich) and were used as received. The reagent norbornene-2-carboxylic acid (Alfa, endo:exo = 75:25) was also used as received.

Physical and Analytical Measurements. ^1H NMR spectra were recorded on a JEOL FX-90Q (FT, 90 MHz), a JEOL FX-270 (FT, 270 MHz), or a Varian XL-400 (FT, 400 MHz) spectrometer. ^1H chemical shifts are reported relative to residual solvent peaks, referenced to 0.00 ppm for $SiMe_4$. All ^1H NMR resonances of uranium complexes are slightly broadened due to the paramagnetism.[19] Infrared spectra were recorded on a Perkin-Elmer 599B spectrometer and were calibrated with polystyrene film. The samples were prepared in the glovebox as mulls with dry, degassed Nujol or degassed Fluorolube and then sandwiched between polished KBr plates in an O-ring-sealed, air-tight holder. Control experiments indicated that the organoactinides did not undergo reaction with Fluorolube on the time scale of the spectroscopic measurements. Cryoscopic molecular weight measurements were carried out in benzene solution with a modified Knauer Type 24.00 instrument calibrated with Cp'_2ThMe_2. Polarimetry measurements were carried out on a Optical Activity Ltd. AA-100 polarimeter. Elemental analyses were performed by Dornis und Kolbe Mikroanalytisches Laboratorium, West Germany, and Oneida Research Service, Inc., Whitesboro, NY.

Synthesis of Sodium (1*R*,2*S*,5*R*)-Menthoxide. A three-neck 500-mL flask equipped with a condenser and a gas inlet was charged with 5.02 g (32.1 mmol) of (1*R*,2*S*,5*R*)-(−)-menthol. Next, the fask was evacuated and backfilled with Ar, and 80 mL of dry toluene was syringed in under an Ar flush. Then, 0.74 g (32.2 mmol) of sodium lumps was added to the solution under an Ar flush. The mixture was refluxed at 110 °C for 40 h. The toluene was then removed in vacuo, and 40 mL of dry pentane was added under an Ar flush. Finally, the pentane was removed in vacuo after stirring, and the resulting white solid was dried in vacuo for 7 h. Yield: 4.55 g, 80%. ^1H NMR (C_6D_6): δ 3.44 (m, 1 H), 2.45 (m, 1 H), 1.99 (m, 1 H), 1.74 (m, 1 H), 1.53–1.69 (m, 2 H), 1.12 (d, 3 H), 1.09 (d, 3 H), 0.98 (d, 3 H), 0.75–1.05 (m, 4 H).

Synthesis of Sodium (*R*)-2-Butoxide. This compound was synthesized in a manner similar to that of sodium (1*R*,2*S*,5*R*)-menthoxide with the use of 1.0 g (13.5 mmol) of (*R*)-(−)-2-butanol and 0.31 g (13.5 mmol) of sodium lumps. The reaction was carried out at room temperature for 1 day and at 110 °C for an additional day. Yield: 0.91 g, 70%. ^1H NMR (C_6D_6): δ 3.95 (m, 1 H), 1.41 (m, 2 H), 1.29 (d, 3 H), 1.06 (t, 3 H).

Synthesis of Sodium [(1*S*)-*endo*]-Bornoxide. A three-neck 500-mL flask equipped with a condenser and a gas inlet was charged with 1.41 g (9.14 mmol) of [(1*S*)-*endo*]-(−)-borneol and then evacuated and backfilled with Ar three times. Next, 100 mL of dry toluene was added under an Ar flush followed by 0.21 g (9.13 mmol) of sodium lumps and 50 μL (1.2 mmol) of methanol. The mixture was stirred at room temperature for 4 h, then at 50 °C for 12 h. After this time, the toluene was removed in vacuo, and 50 mL of pentane was added under an Ar flush. Finally, the pentane was removed in vacuo after stirring, and the resulting white solid was dried in vacuo for several hours. Yield: 1.02 g, 63%. ^1H NMR (C_6D_6): δ 4.18 (m, 1 H), 2.46 (m, 1 H), 2.06 (m, 1 H), 1.82 (m, 1 H), 1.67 (m, 1 H), 1.30 (m, 2 H), 0.95 (br s, 6 H), 0.88 (s, 3 H), 0.77 (m, 1 H), 0.70 (m, 1 H).

Synthesis of Sodium (1*S*,2*S*,5*R*)-Neomenthoxide. This compound was synthesized in a manner similar to that of sodium [(1*S*)-*endo*]-bornoxide with the use of 3.0 g (19.2 mmol) of (1*S*,2*S*,5*R*)-(+)-neomenthol, 0.46 g (20.0 mmol) of sodium lumps, and 20 μL (0.5 mmol) of methanol. The reaction was carried out at 50 °C for 5 h, then at 110 °C for 4 days. Yield: 2.79 g, 82%. ^1H NMR (C_6D_6): δ 4.17 (m, 1 H), 1.63–1.77 (m, 4 H), 1.46 (m, 1 H), 1.25 (m, 3 H), 1.06 (d, 3 H), 0.99 (d, 6 H), 0.82 (m, 1 H).

Synthesis of $Cp'_2Th(n\text{-}Hx)[OCH(t\text{-}Bu)_2]$ (3). In the glovebox, a 30-mL flask was charged with 0.20 g (0.31 mmol) of **2H**. On the vacuum line, toluene (10 mL) and ca. a 10-fold molar excess of 1-hexene were condensed in. The mixture was stirred at 80 °C for 2 days and was then filtered, and the volatiles were removed from the filtrate. Next, 10 mL of pentane was condensed in and then removed in vacuo after stirring and dissolution of the filtrate residue. Drying on the vacuum line for several hours afforded 0.073 g of a white solid. Yield: 32%. ^1H NMR (C_6D_6): δ 3.70 (s, 1 H), 2.05 (s, 30 H), 1.0–2.1 (complex m, 13 H), 1.05 (s, 18 H). IR (Nujol, cm^{-1}): 2733 w, 2045 w, 1367 w, 1162 w, 1052 s, 1000 s, 958 w, 763 w, 652 s, 569 w, 528 w. Anal. Calcd for $C_{35}H_{62}OTh$: C, 57.52; H, 8.55. Found: C, 57.48; H, 8.63.

Synthesis of $Cp'_2U(H)(O\text{-}t\text{-}Bu)$ (4). In the glovebox, a 100-mL flask was charged with 1.54 g (2.36 mmol) of $Cp'_2U(CH_2\text{-}t\text{-}Bu)(O\text{-}t\text{-}Bu)$. On the vacuum line, toluene (40 mL) was condensed in, and then H_2 (1 atm) was introduced. The mixture was stirred at −78 °C for 10 min and then at room temperature overnight. The volatiles were removed in vacuo, pentane (10 mL) was condensed in, and the mixture was filtered. The filtrate was cooled to −78 °C, and cold filtration afforded 0.96 g of a green microcrystalline solid. Yield: 70%. ^1H NMR (C_6D_6): δ 267.1 (s, 1 H), 29.8 (s, 9 H), −1.35 (s, 30 H). IR (Nujol, cm^{-1}): 2733 w, 1363 m, 1263 w, 1232 m, 1184 s, 1022 m, 961 s, 799 w, 780 s, 617 w, 602 w, 523 m, 489 w, 452 w. IR (Fluorolube, cm^{-1}): 2992 s, 2920 s, 2732 w, 1443 m, 1385 m, 1372 m (overlapping with two bands), 1362 m. Anal.

(11) Fendrick, C. M.; Schertz, L. D.; Day, V. W.; Marks, T. J. *Organometallics* **1988**, *7*, 1828–1838.
(12) Lin, Z.; Marks, T. J. *J. Am. Chem. Soc.* **1987**, *109*, 7979–7985.
(13) (a) Conticello, V. P.; Brard, L.; Giardello, M. A.; Tsuji, Y.; Sabat, M.; Marks, T. J. *Abstracts of Papers*, 197th National Meeting of the American Chemical Society, Dallas, TX, April 9–14, 1989; American Chemical Society: Washington, DC, 1989; INOR 31. (b) Conticello, V. P.; Brard, L.; Giardello, M. A.; Tsuji, Y.; Sabat, M.; Marks, T. J. Submitted for publication. (c) Gagné, M. R.; Brard, L.; Conticello, V. P.; Giardello, M. A.; Tsuji, Y.; Marks, T. J. Submitted for publication.
(14) (a) Perrin, D. D.; Armarego, W. L. F.; Perrin, D. R. *Purification of Laboratory Chemicals*, 2nd ed.; Pergamon Press: Oxford, 1980. (b) Adapted from the procedure givein in ref 15.
(15) Moloy, K. G.; Marks, T. J. *J. Am. Chem. Soc.* **1984**, *106*, 7051–7064.
(16) Schrock, R. R.; Fellman, J. D. *J. Am. Chem. Soc.* **1978**, *100*, 3359–3370.
(17) Ketley, A. D.; McClanahan, J. L. *J. Org. Chem.* **1965**, *30*, 942–943.
(18) (a) Wolff, S.; Huecas, M. E.; Agosta, W. C. *J. Org. Chem.* **1982**, *47*, 4358–4359. (b) For preparation of the tosylate, see: Fieser, L. F.; Fieser, M. *Reagents for Organic Synthesis*; Wiley: New York, 1967; Vol. 1, pp 1179–1184.
(19) Fischer, R. D., in ref 3a, Chapter 8.

Calcd for $C_{24}H_{40}OU$: C, 49.48; H, 6.92; MW, 583. Found: C, 48.99; H, 6.54; MW, 581 (cryoscopic in benzene).

Synthesis of Cp′$_2$U(H)[(1*R*,2*S*,5*R*)-menthoxide] (5). In the glovebox, Cp′$_2$UCl$_2$ (0.52 g, 0.90 mmol) was charged into a two-neck 50-mL flask and 0.16 g (0.90 mmol) of sodium (1*R*,2*S*,5*R*)-menthoxide was loaded into an attached addition tube. On the vacuum line, 15 mL of toluene was condensed into the flask and 3 mL into the addition tube. While the Cp′$_2$UCl$_2$ solution was maintained at −78 °C, the contents of the addition tube were poured in. The mixture was stirred at −78 °C for 0.5 h, then at room temperature for 3 h. After the removal of the solvent in vacuo, the crude maroon solid (containing NaCl), Cp′$_2$U(Cl)[(1*R*,2*S*,5*R*)-menthoxide], was dried on the vacuum line overnight.

In the glovebox, a 30-mL flask was charged with the above crude product and 0.10 g (1.1 mmol) of LiCH$_2$TMS. Then, on the vacuum line, 15 mL of toluene was condensed in. The mixture was stirred at −78 °C for 10 min and at room temperature for 3 h. The Ar atmosphere was then replaced with 1 atm of H_2, and the mixture was continuously stirred for 1.5 h. It was then filtered and the residue was washed once with 2 mL of toluene condensed from the bottom part of the frit. Toluene was removed from the filtrate, and 15 mL of pentane was condensed in. After stirring, the pentane was removed in vacuo, and the resulting green solid was dried in vacuo overnight. Total yield: 0.40 g, 67%. ^{1}H NMR (C_6D_6): δ 267.9 (s, 1 H), 87.1 (m, 1 H), 18.3 (m, 1 H), 13.6 (m, 1 H), 13.2 (m, 1 H), 12.5 (m, 1 H), 12.0 (m, 1 H), 10.4 (m, 1 H), 8.31 (m, 1 H), 7.98 (m, 1 H), 4.19 (d, 3 H), 2.94 (d, 3 H), −0.29 (s, 15 H), −0.78 (s, 15 H), −3.43 (d, 3 H), −11.9 (m, 1 H). IR (Nujol, cm^{-1}): 2726 w, 1733 w, 1420 w, 1292 w, 1262 w, 1076 w, 1048 m, 1027 m, 994 w, 921 w, 798 m, 630 m. Anal. Calcd for $C_{30}H_{50}OU$: C, 54.21; H, 7.58. Found: C, 53.73; H, 7.77.

Synthesis of Cp′$_2$U[(1*R*,2*S*,5*R*)-menthoxide]$_2$ (6). In the glovebox, Cp′$_2$U(CH$_2$TMS)$_2$ (1.02 g, 1.50 mmol) and (1*R*,2*S*,5*R*)-(−)-menthol (0.57 g, 3.65 mmol) were combined in a 30-mL flask. On the vacuum line, 20 mL of toluene was condensed in. The mixture was stirred at room temperature for 12 h. Removal of volatiles and vacuum drying afforded 0.91 g of a green solid. Yield: 74%. ^{1}H NMR (C_6D_6): δ 31.6 (m, 2 H), 8.91 (m, 2 H), 5.63 (m, 2 H), 5.08 (m, 4 H), 4.48 (m, 2 H), 4.32 (d, 6 H), 3.43 (m, 2 H), 2.74 (m, 2 H), 2.43 (m, 2 H), 1.82 (d, 6 H), 1.59 (d, 6 H), 0.95 (m, 2 H), −0.48 (s, 30 H). IR (Nujol, cm^{-1}): 2732 w, 1389 m, 1372 m, 1356 w, 1327 w, 1297 w, 1236 w, 1178 w, 1158 w, 1083 m, 1079 m, 1050 s, 1025 s, 996 m, 978 m, 925 m, 876 w, 849 m, 804 w, 768 w, 632 s, 620 s, 529 w, 493 m, 469 w. Anal. Calcd for $C_{40}H_{68}O_2U$: C, 58.66; H, 8.37. Found: C, 58.30; H, 8.65.

Synthesis of Cp′$_2$U(H)[(*R*)-2-butoxide] (7). In the glovebox, a 30-mL flask was charged with 1.0 g (1.7 mmol) of Cp′$_2$UCl$_2$ and 0.16 g (1.7 mmol) of sodium (*R*)-2-butoxide, and 15 mL of toluene was subsequently condensed in on the vacuum line. The mixture was stirred at −78 °C for 10 min, room temperature for 15 h, and then filtered. Toluene was removed from the filtrate in vacuo, and 15 mL of pentane was condensed in. An oily product was obtained even after drying in vacuo overnight. ^{1}H NMR showed the product was Cp′$_2$U(Cl)[(*R*)-2-butoxide]. ^{1}H NMR (C_6D_6): δ 24.2 (m, 1 H), 22.3 (m, 1 H), 20.5 (d, 3 H), 13.6 (m, 1 H), 8.32 (t, 3 H), 2.85 (s, 15 H), 2.64 (s, 15 H).

To the above flask in the glovebox, 0.16 g (1.7 mmol) of LiCH$_2$TMS was added, and then 15 mL of toluene was condensed in on the vacuum line. The mixture was stirred at −78 °C for 10 min and at room temperature for 20 h. The Ar atmosphere was next replaced with H_2, and the reaction mixture was continuously stirred for 5 h. The mixture was then filtered. Toluene was removed from the filtrate in vacuo, and pentane (15 mL) was condensed in. The pentane was removed in vacuo after stirring. A green oily compound was obtained after drying in vacuo overnight. Attempts at recrystallization were unsuccessful. ^{1}H NMR (C_6D_6): δ 265.9 (s, 1 H), 18.2 (m, 1 H), 14.5 (m, 1 H), 13.9 (d, 3 H), 3.29 (m, 1 H), 0.61 (t, 3 H), −0.35 (s, 15 H), −0.61 (s, 15 H). IR (Nujol, cm^{-1}): 2731 w, 2092 w, 1494 w, 1339 w, 1251 m, 1161 m, 1130 s, 1034 s, 996 s, 970 w, 926 s, 856 w, 822 m, 775 m.

Synthesis of Cp′$_2$U(H)[(1*S*)-*endo*]-bornoxide (8). In the glovebox, a 30-mL flask was charged with 1.0 g (1.7 mmol) of Cp′$_2$UCl$_2$ and 0.30 g (1.7 mmol) of sodium [(1*S*)-*endo*]-bornoxide. Next, 15 mL of toluene was condensed in on the vacuum line. The mixture was stirred at −78 °C for 0.5 h, at room temperature for 4 h, and was then filtered. Toluene was removed from the filtrate in vacuo, and 15 mL of pentane was condensed in. The resulting pentane solution was then slowly cooled to −78 °C. Cold filtration (−78 °C) and vacuum drying afforded crude Cp′$_2$U(Cl)[(1*S*)-*endo*]-bornoxide as an orange solid. Yield: 0.99 g, 82%.

In the glovebox, a 30-mL flask was charged with 0.39 g (0.56 mmol) of Cp′$_2$U(Cl)[(1*S*)-*endo*]-bornoxide and 0.06 g (0.64 mmol) of LiCH$_2$TMS, and 15 mL of toluene was condensed in on the vacuum line. The mixture was stirred at −78 °C for 10 min and at room temperature for 18 h. Next, the Ar atmosphere was replaced by H_2. The mixture was continuously stirred for 1.5 h and then filtered. Toleune was removed from the filtrate in vacuo, and 15 mL of pentane was condensed in. The resulting pentane solution was then slowly cooled to −78 °C. Cold filtration (−78 °C) and vacuum drying afforded 0.22 g of a green solid. Yield: 59%. ^{1}H NMR (C_6D_6): δ 269.6 (s, 1 H), 115.9 (m, 1 H), 26.7 (m, 1 H), 20.3 (m, 1 H), 17.1 (s, 3 H), 13.4 (m, 1 H), 12.3 (s, 3 H), 10.3 (m, 1 H), 8.04 (s, 3 H), 7.17 (m, 1 H), 6.62 (m, 1 H), 5.71 (m, 1 H), −0.24 (s, 15 H), −1.82 (s, 15 H). IR (Nujol, cm^{-1}): 2730 w, 1307 w, 1236 w, 1208 w, 1165 w, 1139 w, 1110 m, 1081 m, 1061 s, 1033 s, 1022 m, 994 w, 979 w, 950 w, 932 w, 918 w, 883 w, 835 m, 799 w, 776 w, 662 m, 619 s, 598 m, 520 w, 490 w, 453 w. IR (Fluorolube, cm^{-1}): 2923 s, 2732 w, 1488 w, 1442 m, 1400 m, 1363 m. Anal. Calcd for $C_{30}H_{48}OU$: C, 54.37; H, 7.30; MW, 663. Found: C, 53.88; H, 7.61; MW, 714 (cryoscopic in benzene).

Synthesis of Cp′$_2$Th(H)[(1*S*)-*endo*]-bornoxide (9). This compound was synthesized in a manner similar to **8** with 0.47 g (0.82 mmol) of Cp′$_2$ThCl$_2$, 0.15 g (0.85 mmol) of sodium [(1*S*)-*endo*]-bornoxide, 0.080 g (0.85 mmol) of LiCH$_2$TMS, and H_2 gas. Cold filtration afforded 0.40 g of a white solid. Total yield: 74%. ^{1}H NMR (C_6D_6): δ 17.7 (s, 1 H), 4.57 (m, 1 H), 2.39 (m, 1 H), 2.23 (m, 1 H), 2.15 (s, 15 H), 2.13 (s, 15 H), 1.72 (m, 1 H), 1.56 (m, 1 H), 1.35 (m, 1 H), 1.20 (m, 1 H), 1.04 (m, 1 H), 0.95 (s, 3 H), 0.82 (s, 6 H). IR (Nujol, cm^{-1}): 2728 w, 1426 w, 1348 m, 1234 w, 1203 w, 1164 w, 1137 w, 1110 s, 1082 m, 1064 s, 1033 m, 1021 w, 992 w, 918 w, 882 w, 836 m, 798 w, 660 m, 612 m, 542 m, 439 w. IR (Fluorolube, cm^{-1}): 2932 s, 2722 w, 1440 m, 1386, 1338 m. Anal. Calcd for $C_{30}H_{48}OTh$: C, 54.87; H, 7.37. Found: C, 54.55; H, 7.21.

Synthesis of Cp′$_2$U(H)[(1*S*,2*S*,5*R*)-neomenthoxide] (10). This compound was synthesized in a manner similar to **8** with 0.81 g (1.4 mmol) of Cp′$_2$UCl$_2$, 0.26 g (1.5 mmol) of sodium (1*S*,2*S*,5*R*)-neomenthoxide, 0.15 g (1.6 mmol) of LiCH$_2$TMS, and H_2 gas. Green solids were isolated. Total yield: 0.62 g, 67%. ^{1}H NMR (C_6D_6): δ 269.2 (s, 1 H), 127.6 (m, 1 H), 42.2 (m, 1 H), 36.5 (m, 1 H), 34.5 (m, 1 H), 14.7 (m, 1 H), 13.3 (m, 1 H), 11.6 (m, 1 H), 10.5 (d, 3 H), 6.63 (m, 1 H), 6.09 (m, 1 H), 3.49 (m, 1 H), 1.36 (d, 3 H), 1.08 (d, 3 H), −1.43 (s, 15 H), −1.78 (s, 15 H). IR (Nujol, cm^{-1}): 2733 w, 1736 w, 1415 m, 1369 m, 1273 w, 1252 w, 1223 m, 1199 m, 1155 s, 1102 w, 1060 m, 1031 s, 994 m, 966 s, 941 s, 890 s, 853 s, 817 m, 798 w, 759 w, 701 s, 613 w, 542 m, 497 s. IR (Fluorolube, cm^{-1}): 2920 s, 2738 w, 1459 m, 1387 m, 1370 m. Anal. Calcd for $C_{30}H_{50}OU$: C, 54.21; H, 7.58. Found: C, 53.88; H, 7.69.

Kinetic Studies of Olefin Insertion Reactions. In a typical experiment, a Teflon-valved 5-mm NMR tube was charged in the glovebox with carefully measured quantities of the actinide hydride complex (ca. 10 mg, 15 μmol) and the olefin in at least 20-fold molar excess dissolved in 0.50 mL of toluene-d_8. Then the NMR tube was removed from the glovebox and immediately immersed in a constant-temperature bath that was usually set to 60.0 ± 0.1 °C. At measured time intervals, the NMR tube was inserted into the probe of the XL-400 NMR spectrometer and an ^{1}H spectrum recorded. A long pulse delay (ca. 5T_1) was employed to avoid saturation. No observable reaction was noted during the data accumulation period at 20 °C. The kinetics were usually monitored from the intensities of ^{1}H NMR signals of the metal hydride complexes over approximately 3 half-lives.

The concentration of the hydride, C, was measured by the Cp′ peak (or other peak) area A_H standardized to the residual solvent peak area A_S ($C = A_H/A_S$) by the integration subroutine of the instrument. All data collected for the olefin insertion reactions could be fit by least-squares to eq 2,[20] where C_0 is the initial concentration of the hydride. Standard deviations in the rate constants are derived from the fitting procedure.

$$\ln (C_0/C) = k't \qquad (2)$$

^{1}H NMR Studies of Diastereoselectivities of Prochiral Olefin or Ketone Insertion Reactions with Chiral Actinide Hydride Complexes. In studies of diastereoselectivities of prochiral olefin or ketone insertion into the actinide–hydride bonds of complexes with chiral alkoxide ancillary ligands, ca. 10 mg (15 μmol) of the actinide complex and ca. 50 μmol of the olefin or ketone were dissolved in 0.5 mL of C_6D_6. The insertion products were identified primarily by ^{1}H NMR spectroscopy. The magnetically nonequivalent Cp′ ^{1}H NMR signals of each of the two diastereomers (diastereomer A refers to the major product, B to the minor product) were used to calculate the diasteromeric excess of the olefin insertion reaction. Low-temperature experiments were carried out in toluene-d_8 with a Neslab PBC-4II refrigerated bath.

Identification of Cp′$_2$U(*exo*-2-norbornyl)[(1*S*)-*endo*]-bornoxide (11). The reaction of norbornene with **8** afforded **11** within 1 h at room tem-

(20) Moore, J. W.; Pearson, R. G. *Kinetics and Mechanism*, 3rd ed.; Wiley-Interscience: New York, 1981; Chapter 3.

perature. ^{1}H NMR (C_6D_6): diastereomer A, δ 25.6 (m, 1 H), 25.3 (m, 1 H), 20.0 (m, 1 H), 16.3 (s, 3 H), 15.1 (s, 3 H), 14.0 (m, 1 H), 10.5 (m, 1 H), 9.51 (m, 1 H), 8.92 (s, 3 H), 2.53 (m, 1 H), 2.30 (s, 15 H), 1.10 (s, 15 H), 0.93 (m, 1 H), −10.7 (m, 2 H), −12.4 (m, 1 H), −13.5 (m, 1 H), −14.3 (m, 1 H), −14.9 (m, 1 H), −18.9 (m, 1 H), −20.3 (m, 1 H), −32.8 (m, 1 H); diastereomer B, δ 28.6 (m, 1 H), 27.2 (m, 1 H), 21.5 (m, 1 H), 15.6 (s, 3 H), 15.3 (s, 3 H), 14.7 (m, 1 H), 10.0 (m, 1 H), 9.87 (m, 1 H), 9.09 (s, 3 H), 2.04 (m, 1 H), 1.88 (m, 1 H), 1.70 (s, 15 H), 1.46 (s, 15 H), −5.28 (m, 2 H), −11.6 (m, 1 H), −13.1 (m, 1 H), −14.7 (m, 1 H), −19.0 (m, 1 H), −19.7 (m, 1 H), −20.2 (m, 1 H), −30.3 (m, 1 H).

Identificiation of Cp'_2Th(*exo*-2-norbornyl){[(1*S*)-*endo*]-bornoxide} (12). The reaction of norbornene with **9** afforded **12** within 1 h at room temperature. ^{1}H NMR (C_6D_6, diagonstic resonances): diastereomer A, δ 2.060 (s, 15 H), 2.037 (s, 15 H), 0.98 (s, 6 H), 0.85 (s, 3 H); diastereomer B, δ 2.070 (s, 15 H), 2.042 (s, 15 H), 0.86 (s, 3 H), 0.84 (s, 6 H).

Identification of Cp'_2U(*exo*-2-norbornyl)[(1*R*,2*S*,5*R*)-menthoxide] (13). The reaction of norbornene with **5** afforded **13** within 12 h at room temperature. ^{1}H NMR (C_6D_6): diastereomer A, δ 14.8 (m, 1 H), 12.6 (m, 1 H), 12.0 (m, 1 H), 10.5 (m, 1 H), 10.2 (d, 3 H), 5.28 (d, 3 H), 4.74 (m, 1 H), 4.39 (m, 1 H), 3.71 (d, 3 H), 3.46 (m, 1 H), 2.88 (m, 1 H), 1.82 (m, 1 H), 1.67 (s, 15 H), 1.59 (s, 15 H), −1.82 (m, 1 H), −2.86 (m, 1 H), −6.07 (m, 1 H), −6.92 (m, 1 H); diastereomer B, δ 15.4 (m, 1 H), 12.3 (m, 1 H), 11.6 (m, 1 H), 10.3 (d, 3 H), 10.1 (m, 1 H), 5.13 (m, 1 H), 4.67 (d, 3 H), 4.26 (m, 1 H), 4.14 (m, 1 H), 4.00 (d, 3 H), 2.59 (m, 1 H), 2.04 (s, 15 H), 1.75 (m, 1 H), 1.38 (s, 15 H), −1.63 (m, 1 H), −2.57 (m, 1 H), −5.83 (m, 1 H), −6.39 (m, 1 H).

Identification of Cp'_2U(*s*-Bu)[(1*R*,2*S*,5*R*)-menthoxide] (14). The reaction of *cis*-2-butene with **5** initially afforded **14**, which isomerized to Cp'_2U(*n*-Bu)[(1*R*,2*S*,5*R*)-menthoxide] (**15**) (vide infra) in 1 day at room temperature. ^{1}H NMR (C_6D_6, diagnostic resonances): diastereomer A, δ 10.9 (d, 3 H), 3.81 (d, 3 H), 0.62 (s, 15 H), 0.24 (s, 15 H), −15.2 (t, 3 H); diastereomer B, δ 10.4 (d, 3 H), 4.02 (d, 3 H), 0.86 (s, 15 H), 0.67 (s, 15 H), −14.6 (t, 3 H).

Identification of Cp'_2U(*n*-Bu)[(1*R*,2*S*,5*R*)-menthoxide] (15). The reaction of 1-butene with **5** afforded **15** within 20 min at room temperature. ^{1}H NMR (C_6D_6): δ 91.2 (m, 1 H), 26.7 (m, 1 H), 21.0 (m, 1 H), 20.5 (m, 1 H), 16.6 (m, 1 H), 15.9 (m, 1 H), 13.8 (m, 1 H), 11.0 (m, 1 H), 10.2 (m, 1 H), 9.87 (m, 1 H), 8.79 (d, 3 H), 4.75 (d, 3 H), 1.73 (d, 3 H), 0.88 (s, 15 H), 0.57 (s, 15 H), −11.8 (t, 3 H), −20.8 (m, 2 H), −26.3 (m, 1 H), −28.0 (m, 1 H), −186.7 (m, 1 H), −190.2 (m, 1 H).

Identification of Cp'_2U[OCHPh(Me)][(1*R*,2*S*,5*R*)-menthoxide] (16). The reaction of MeC(O)Ph with **5** afforded **16** within 1 h at room temperature. ^{1}H NMR (C_6D_6, diagnostic resonances): diastereomer A, δ 2.48 (d, 3 H), 1.57 (d, 3 H), 1.36 (d, 3 H), 1.14 (d, 3 H), 0.12 (s, 15 H), −0.23 (s, 15 H); diastereomer B, δ 2.60 (d, 3 H), 1.66 (d, 3 H), 0.07 (s, 15 H), −0.09 (s, 15 H), −0.39 (d, 3 H), −0.47 (d, 3 H).

Identification of Cp'_2U[OCHPh(C_3H_7)][(1*R*,2*S*,5*R*)-menthoxide] (17). The reaction of C_3H_7C(O)Ph with **5** afforded **17** within 1 h at room temperature. ^{1}H NMR (C_6D_6, diagnostic resonances): diastereomer A, δ 0.06 (s, 15 H), −0.16 (s, 15 H); diastereomer B, 0.01 (s, 15 H), −0.14 (s, 15 H).

Identification of Cp'_2U(*exo*-2-norbornyl)[(*R*)-2-butoxide] (18). The reaction of norbornene with **7** afforded **18** at room temperature in 20 min. ^{1}H NMR (C_6D_6, diagnostic resonances): diastereomers A and B, δ 26.3 (m, 1 H), 25.9 (m, 1 H), 25.6 (d, 3 H), 25.5 (d, 3 H), 13.3 (t, 3 H), 13.2 (t, 3 H), 1.59 (s, 15 H), 1.55 (s, 15 H), 1.31 (s, 15 H), 1.30 (s, 15 H).

Identification of Cp'_2U(*exo*-2-norbornyl)[(1*S*,2*S*,5*R*)-neomenthoxide] (19). The reaction of norbornene with **10** at room temperature for 4 days afforded **19** with 70% completion. ^{1}H NMR (C_6D_6, diagnostic resonances): diastereomer A, δ 11.3 (d, 3 H), 5.27 (d, 3 H), 4.89 (d, 3 H), 2.48 (s, 15 H), 0.34 (s, 15 H); diastereomer B, δ 9.12 (d, 3 H), 5.49 (d, 3 H), 4.53 (d, 3 H), 2.59 (s, 15 H), 0.66 (s, 15 H).

Identification of Cp'_2Th(*s*-Bu)(*O*-*t*-Bu) (20). The reaction of *cis*-2-butene with **1H** initially afforded **20**, which then isomerized to Cp'_2Th(*n*-Bu)(O-*t*-Bu) (**21**) (vide infra) within 3 days at room temperature. ^{1}H NMR (C_6D_6): δ 2.03 (s, 30 H), 1.73 (br m, 2 H), 1.70 (d, 3 H), 1.32 (t, 3 H), 1.27 (s, 9 H), 0.25 (br m, 1 H).

Identification of Cp'_2Th(*n*-Bu)(*O*-*t*-Bu) (21). The reaction of 1-butene with **1H** afforded **21** within 1 h at room temperature. ^{1}H NMR (C_6D_6): δ 2.02 (s, 30 H), 1.96 (br m, 2 H), 1.66 (m, 2 H), 1.25 (s, 9 H), 1.20 (t, 3 H), 0.56 (br m, 2 H).

Reaction of 11 with CO_2 and then HCl. In the glovebox, a 30-mL flask was charged with 0.28 g (3.0 mmol) of norbornene and 0.60 g (0.91 mmol) of **8**, and 15 mL of toluene was condensed in on the vacuum line. The mixture was stirred at room temperature for 4 h, and then the volatiles were removed in vacuo. After this, 15 mL of toluene was condensed in, and CO_2 gas was introduced into the reaction flask. The mixture was stirred overnight, and then the volatiles were removed in vacuo. Next, 5 mL of 3 N aqueous HCl was added to the resulting products, and the mixture was stirred for 3 h. The mixture was then extracted with 3 × 15 mL of Et_2O. The combined ether extracts were then extracted with 10 mL of 1 N NaOH and separated. The alkaline aqueous solution was next washed with 3 × 15 mL of Et_2O, acidified with 3 N HCl, and extracted with 3 × 15 mL of Et_2O. Evaporation of the combined Et_2O extracts afforded two enantiomers of *exo*-norbornane-2-carboxylic acid, which exhibited an ^{1}H NMR spectrum identical with that of an authentic sample of *exo*-norbornane-2-carboxylic acid (Alfa, endo:exo = 75:25) and in good agreement with that reported in the literature.[21a] Polarimetric measurements[21b] in EtOH identified [(1*R*,2*R*,4*S*)-*exo*]-(−)-norbornane-2-carboxylic acid as the major enantiomer with 21% ee. ^{1}H NMR (acetone-d_6): δ 2.48 (m, 1 H), 2.31 (m, 1 H), 2.24 (m, 1 H), 1.80 (m, 1 H), 1.45 (br m, 3 H), 1.20 (br m, 3 H).

Table I. Metal–Hydride Vibrational Modes for Organoactinide Hydrides

complex	ν_{M-H} (ν_{M-D}), cm^{-1}	reference
Cp'_2U(H)(O-*t*-Bu) (4)	1372	this work
Cp'_2U(H){[(1*S*)-*endo*]-bornoxide} (8)	1363	this work
Cp'_2Th(H){[(1*S*)-*endo*]-bornoxide} (9)	1348	this work
Cp'_2U(H)[(1*S*,2*S*,5*R*)-neomenthoxide] (10)	1370	this work
$[Cp'_2Th(\mu\text{-}H)H]_2$	1404[a] (1002) 1370[a] (979) 1215 (873) 1114 (609) 650 (465)	4c
$[Cp'_2U(\mu\text{-}H)H]_2$	1335[a] 1180	4c
Cp'_2Th(H)(O-*t*-Bu)	1359[a] (981)	4c
Cp'_2Th(H)(OCH-*t*-Bu_2)	1355[a] (971)	15
Cp'_2U(H){OSi[C(CH$_3$)$_3$](Me)$_2$}	1395 (988)	9c
$[(Me_3Si)_2N]_3ThH$	1480[a] (1060)	31
$[(Me_3Si)_2N]_3UH$	1430[a] (1020)	31

[a] Assigned to a mode that is predominantly terminal M–H stretching character.

Molecular Mechanics and Graphics Studies. Molecular mechanics calculations for the interaction of **8** with norbornene were carried out with the Dreiding and MMP2 force field options of the BIOGRAF software package[22,23] implemented on a microVAX 2000 with an Evans and Sutherland PS390 graphics system. The goal of this study was to examine the *relative* steric energetics (primarily olefin–ligand repulsive) of various olefin approach trajectories toward the U center. The potential energy in such a calculation is expressed as a sum of bonded and nonbonded interactions, specifically: bond stretching, angle bending, dihedral angle torsion, inversion, and van der Waals interactions.[22]

In setting up a model potential for the Cp'_2U(H)OR* molecular structure, it was recognized that, for a large data base of Cp'_2AnX_2 compounds, metrical features such as ∠ring centroid–An–ring centroid, ∠X–An–X, *d*(average) An–C(Cp') distance, and the disecting of ∠ring centroid–An–ring centroid by the perpendicular AnX_2 plane ("equatorial girdle") are essentially invariant.[4e,b,11,24] Parameters for the Cp'_2U(H)O– fragment of **8** were taken from the crystallographic data for $[Cp'_2U(OMe)]_2PH$.[25] The U–H bond distance (1.98 Å) was estimated from a neutron diffraction derived terminal Th–H bond distance (2.03 Å)[26] corrected for the difference in metal ion radii.[27] The norbornene and [(1*S*)-*endo*]-bornyl moieties were constructed, and the energies were

(21) (a) Wersiuk, N. H. *Can. J. Chem.* **1975**, *53*, 26–40. (b) $[\alpha]^{20}_D$ = −27.8° for [(1*R*,2*R*,4*S*)-*exo*]-(−)-norbornane-2-carboxylic acid (in EtOH), see: Berson, J. A.; Ben-Efraim, D. A. *J. Am. Chem. Soc.* **1959**, *81*, 4083–4087.

(22) Mayo, S. L.; Olafson, B. D.; Goddard, W. A., III. *BIOGRAF Version 1.50 Reference Manual*; BioDesign, Inc.: Pasadena, CA, 1988; Appendix G.

(23) For recent molecular modeling applications of this software package (or earlier versions), see: (a) Bowler, B. E.; Meade, T. J.; Mayo, S. L.; Richards, J. H.; Gray, H. B. *J. Am. Chem. Soc.* **1989**, *111*, 8757–8759. (b) Naylor, A. M.; Goddard, W. A., III. *ACS Symp. Ser.* **1989**, *No. 392*, 65–87. (c) Naylor, A. M.; Goddard, W. A., III; Tomalia, D. A.; Kiefer, G. B. *J. Am. Chem. Soc.* **1989**, *111*, 2339–2341. (d) Karasawa, N.; Goddard, W. A., III. *J. Phys. Chem.* **1988**, *92*, 5828–5832.

(24) (a) Marks, T. J.; Streitwieser, A., Jr. in ref 4a, Chapter 22. (b) Bruno, J. W.; Smith, G. M.; Marks, T. J.; Fair, C. K.; Schultz, A. J.; Williams, J. M. *J. Am. Chem. Soc.* **1986**, *108*, 40–56. (c) Bruno, J. W.; Marks, T. J.; Day, V. W. *J. Organomet. Chem.* **1983**, *250*, 237–246. (d) Eigenbrot, C. W., Jr.; Raymond, K. N. *Inorg. Chem.* **1982**, *21*, 2653–2660.

(25) Duttera, M. R.; Day, V. W.; Marks, T. J. *J. Am. Chem. Soc.* **1984**, *106*, 2907–2912.

(26) Broach, R.; Schultz, A. J.; Williams, J. M.; Brown, G. M.; Manriquez, J. M.; Fagan, P. J.; Marks, T. J. *Science* **1979**, *203*, 172–174.

(27) Shannon, R. D. *Acta Crystallogr.* **1976**, *A32*, 751–767.

Chart I. Chiral Alcohols Used

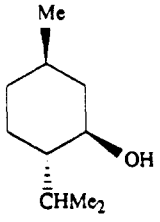

(1R,2S,5R)-(-)-Menthol

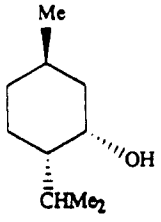

(1S,2S,5R)-(+)-Neomenthol

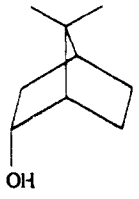

[(1S)-*endo*]-(-)-Borneol

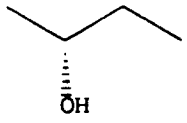

(R)-(-)-2-Butanol

minimized with the Dreiding force field. The organoactinide structure was then obtained by docking the bornyl fragment to the $Cp'_2U(H)(O)$- fragment with a C–O distance of 1.44 Å and a U–O–C angle of 178°.[25] The energy of the alkoxy portion was minimized again. Next, the optimum geometry for the $Cp'_2U(H)OR^*$ complex was estimated by allowing rotation about the O–C(bornyl) bond to occur (with fixed ∠O–U–H and ∠ring centroid–U–ring centroid) until an energy minimum (212.1 kcal/mol) was reached. For these latter calculations, U–O and U–H stretching force constants of 317.8 and 158.2 kcal/mol·Å^2, respectively, were estimated from the A_{1g} U–O stretching mode of $U(O\text{-}CH_3)_6$ (500 cm^{-1}, confirmed by ^{18}O substitution)[28] and the U–H stretching mode of **8** (1363 cm^{-1}, confirmed by ^2H substitution; Table I). The O–U–H bending force constant was estimated to be 100 kcal/mol by standard approximations for nonlinear triatomics.[29] The Lennard-Jones 12-6 van der Waals potential for uranium was estimated with the published U–U bond enthalpy[30a] of 53 kcal/mol and U–U bond length[30b] of 2.77 Å.

In analyzing the relative energetics of olefin approach trajectories toward the U center, the olefin face was constrained to lie over the U–H bond with the norbornene C=C bond vector coplanar with the O–U–H equatorial girdle and the plane defined by C (bridgehead), C=C, C (bridgehead) perpendicular to the approach vector. Calculations were carried out along three pathways (A–C) in which norbornene could

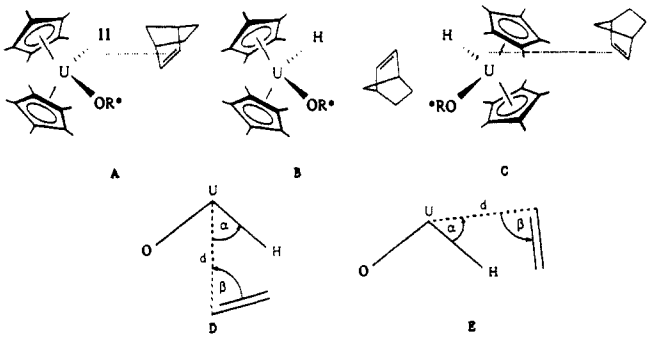

approach for subsequent insertion. Suitable variation of α and β parameters allowed simulation of olefin approach toward an initial π complex or direct addition to the U–H bond. Such distinctions were blurred at distances for which olefin–ligand repulsions were already substantial. The distance d was varied from 7 to 5 Å, and angles α and β were varied from 50° to 60° and 100° to 120°, respectively. These values were chosen for closest examination after initial, survey calculations indicated that major departures from these values resulted in energetically or chemically unrealistic results (higher α values invariably led to severe OR*–olefin repulsions while lower α values led to pathways not readily identifiable with complexation or insertion processes). For each trial set of d, α, and β parameters, the lowest energy was obtained by allowing the alkoxy ligand to rotate about the C–O bond (intervals of 10°) and by allowing rotating the Cp′ ligands to rotate about around the ring centroid–U vectors (intervals of 18°) with the SEARCH subroutine of the program. Calculations indicated that energies of the trial pathways were always shifted to the same extent (within 1 kcal/mol) when the uranium force field was varied. Although the U–H and U–O bond distances and the H–U–O bond angle were fixed during specific calculations, variation of the force constants by ±50% did not significantly change the results. Likewise, variation of van der Waals energy terms for uranium by ±20% affected all calculations to the same extent (within 1 kcal/mol). Decreasing the U–O–C angle to 150° resulted in a 120 kcal/mol *increase* in the minimized energy. Non-van der Waals contributions to the total energies never exceeded 40 kcal/mol.

Results

Synthesis and Properties of Organoactinide Hydrides. Chiral sodium alkoxides can be synthesized directly via the reaction of sodium with the corresponding alcohols (eq 3). For sterically

$$Na + R^*OH \xrightarrow{\text{toluene}} NaOR^* + \tfrac{1}{2}H_2 \quad (3)$$

R* = (1*R*,2*S*,5*R*)-menthyl, (*R*)-2-butyl

$$Na + MeOH \xrightarrow{\text{toluene}} NaOMe + \tfrac{1}{2}H_2 \quad (4)$$

$$NaOMe + R^*OH \xrightarrow{\text{toluene}} NaOR^* + MeOH \quad (5)$$

R* = [(1*S*)-*endo*]-bornyl, (1*S*,2*S*,5*R*)-neomenthyl

encumbered alcohols, a trace amount of methanol is needed to catalyze the reaction (presumably via eqs 4 and 5). The methodology used to synthesize actinide alkoxide hydrides is well documented.[14b,15] The dichloro complexes are first treated with 1 equiv of chiral sodium alkoxide (Chart I) and then with $LiCH_2TMS$ in toluene.[31] Further reaction with H_2 (or D_2) affords desired hydride (or deuteride) complexes (eqs 6–8). In contrast,

$$Cp'_2AnCl_2 + NaOR/R^* \xrightarrow{\text{toluene}} Cp'_2An(Cl)(OR/R^*) + NaCl \quad (6)$$

$$Cp'_2An(Cl)(OR/R^*)(OR/R^*) + LiCH_2TMS \xrightarrow{\text{toluene}} Cp'_2An(CH_2TMS)(OR/R^*) + LiCl \quad (7)$$

$$Cp'_2An(CH_2TMS)(OR/R^*) + H_2 \xrightarrow{\text{toluene}} Cp'_2An(H)(OR/R^*) + TMS \quad (8)$$

1,2,4,5,7–10

1: An = Th, OR = *tert*-butoxide
2: An = Th, OR = $OCH(t\text{-}Bu)_2$
4: An = U, OR = *tert*-butoxide
5: An = U, OR* = (1*R*,2*S*,5*R*)-menthoxide
7: An = U, OR* = (*R*)-2-butoxide
8: An = U, OR* = [(1*S*)-*endo*]-bornoxide
9: An = Th, OR* = [(1*S*)-*endo*]-bornoxide
10: An = U, OR* = (1*S*,2*S*,5*R*)-neomenthoxide

when $(Cp'_2UH_2)_2$ or $Cp'_2U(CH_2TMS)_2$ is treated with 1 equiv of (1*R*,2*S*,5*R*)-(–)-menthol, a mixture of mono- and dimenthoxide complexes is obtained. All newly synthesized organoactinides were characterized by standard spectroscopic/analytical techniques (see Experimental Section for details). Due to the paramagnetism of the $5f^2$ uranium(IV) center and the rapid electron spin–lattice relaxation times, magnetically nonequivalent ligand protons are generally well-separated and can be readily resolved in the ^1H NMR spectra.

Complete infrared spectroscopic data for the actinide hydride complexes are given in the Experimental Section. By comparing the hydride alkoxide IR data with those of known actinide hydrides and those of the parent alcohols, and by also comparing the thorium hydrides with the analogous uranium hydrides (e.g., **1H**

(28) Cuellar, E. A.; Miller, S. S.; Marks, T. J.; Weitz, E. *J. Am. Chem. Soc.* **1983**, *105*, 4580–4589.

(29) (a) For typical nonlinear Y–X–Y molecules, $k_{Y\text{-}X\text{-}Y}/l^2 \approx 0.1k_{X\text{-}Y}$ where l is the bond length for X–Y.[29b] (b) Herzberg, G. *Molecular Spectra and Molecular Structure. II. Infrared and Raman Spectra of Polyatomic Molecules*; Van Nostrand Reinhold New York, 1945; p 170.

(30) (a) *CRC Handbook of Chemistry and Physics*, 69th ed.; Weast, R. C., Astle, M. J., Beyer, W. H., Eds.; CRC Press: Boca Raton, FL, 1988; p F-177. (b) Reference 30a, p F-166.

(31) The reaction of $LiCH_2$-*t*-Bu with uranium complexes does not yield the expected alkyl complexes, probably due to the reduction of U(IV).

versus 4), the actinide–hydride vibrational modes[4,9d,11,32] can be readily discerned. Assignments are given in Table I along with selected literature data. All the newly identified M–H stretching frequencies are in the range of 1348–1372 cm^{-1}, which is typical of terminal actinide–hydride complexes (1300–1500 cm^{-1}). The monomeric character of these hydrides is also supported by cryoscopic molecular weight measurements.

Kinetic Studies of Olefin Insertion. Cryoscopic molecular weight measurements established the monomeric character of compounds **1**, **2**,[33] **4**, and **8** in benzene. Therefore, all hydride complexes used in the present kinetic studies are assumed to be monomeric. All of the hydride complexes investigated cleanly undergo olefin insertion to form the corresponding alkyl complexes (eq 9).[4] This

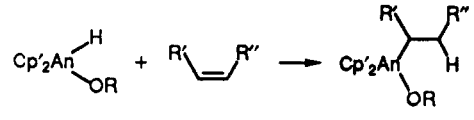

(9)

process is accompanied by expected ^1H NMR Cp′ and An–H spectral changes.[4,12,15] For the uranium complexes, typical green hydride to brown alkyl color changes[4c,12] are also observed. In all cases, the resulting alkyls are known compounds or can be straightforwardly identified by ^1H NMR techniques. Insertion reactions for **1H** were followed by monitoring ^1H *t*-Bu signals, for **2** by monitoring hydride or methine proton signals,[34] and for **4** by monitoring Cp′ signals. Kinetic measurements were carried out over at least 3 half-lives. In the presence of an at least 20-fold molar excess of olefin, all reactions were determined to be first order in organoactinide complex. In the case of **1H** + cyclohexene, the rate constants obtained from both reactant and product *t*-Bu signals agreed to within experimental error, indicating that no significant competing reactions are involved.

As noted in the Experimental Section, the initial reaction of *cis*-2-butene with **1H** initially gave the expected *sec*-butyl complex. However, over a period of 3 days at room temperature, the product was observed to undergo isomerization to the more stable *n*-butyl complex (eq 10), $k \approx 1 \times 10^{-5}\ s^{-1}$. The identity of the final product

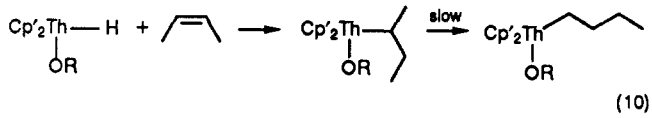

(10)

was further confirmed by noting that the same product is obtained in the reaction of 1-butene with **1H**. Both complexes were additionally characterized by ^1H homonuclear decoupling experiments. The reaction of **5** and *cis*-2-butene proceeds similarly, and the *sec*-butyl → *n*-butyl isomerization occurs with $k \approx 3 \times 10^{-5}\ s^{-1}$. In neither of the isomerization reactions could free 1-butene be detected in concurrently recorded ^1H NMR spectra (≲5% of the M-alkyl concentration). Reasonably assuming that the isomerization proceeds via β-H elimination/readdition (eq 11),[6,7]

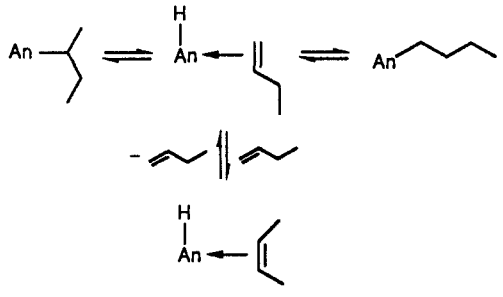

(11)

this result indicates that little 1-butene escapes the actinide coordination sphere. However, it is not clear whether the reasons

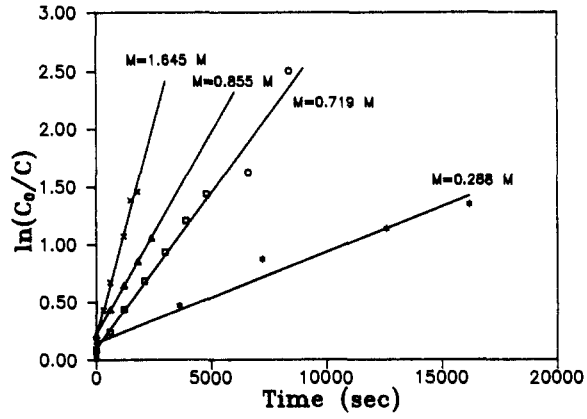

Figure 1. Kinetic plots for the reaction (insertion) of cyclohexene with $Cp'_2Th(H)(O\text{-}t\text{-}Bu)$ (**1H**) at various olefin concentrations (60 °C).

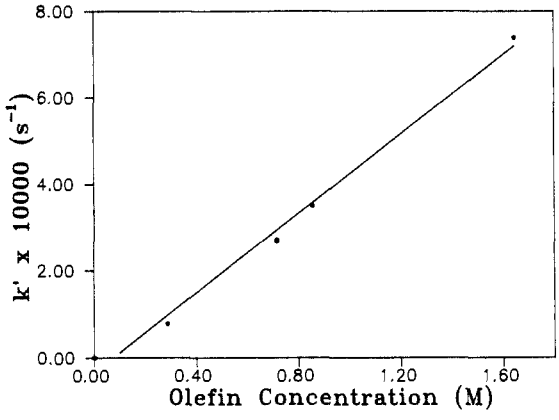

Figure 2. Plot of the observed pseudo-first-order rate constant k' versus olefin concentration for the reaction of cyclohexene with $Cp'_2Th(H)(O\text{-}t\text{-}Bu)$ (**1H**).

are kinetic, having to do with the lifetime (intramolecular insertion is far more rapid than olefin exchange), or thermodynamic, reflecting the stability (the 1-butene binding constant is far greater than that of other butenes) of the putative, intermediate hydride olefin complex (eq 11). We show elsewhere that, as detected by NMR spectroscopy, organolanthanide–olefin complexation is weak and kinetically labile.[35] In regard to bonding energetics, the isomerization result indicates that the *n*-butyl isomer is the more thermodynamically favored.

The reaction of **1H** + cyclohexene was also investigated with varying concentrations of olefin. Figure 1 shows kinetic plots for these reactions. A plot of the observed pseudo-first-order rate constants k' versus the olefin concentrtion gives a straight line (Figure 2). These results are consistent with a second-order rate law as in eq 12, i.e., first order in the hydride and first order in

$$\text{rate} = k'[\text{An–H}] = k[\text{olefin}][\text{An–H}] \qquad (12)$$

the olefin. Since the olefin insertion chemistry is rather similar for all tetravalent organoactinide hydrides,[4] it is reasonable to assume that the other monomeric hydrides also undergo olefin insertion according to a second-order rate law. Listed in Table II are second-order rate constant data for the systems studied in the present investigation. There was no reaction observed after heating a mixture of **2H** + cyclohexene at 60 °C for 1 week. In contrast, the reactions of **1H** and **4** with styrene and 1-hexene were too rapid to study accurately by ^1H NMR techniques at room temperature. The rate constants are estimated to be greater than $10^{-2}\ M^{-1}\ s^{-1}$ assuming the reaction half-lives are less than 2 min at 0.5 M concentration of the olefin. The rate of ethylene reaction is necessarily an estimate because the concentration of ethylene

(32) Turner, H. W.; Simpson, S. J.; Andersen, R. A. *J. Am. Chem. Soc.* **1979**, *101*, 2782.

(33) A cryoscopic molecular weight measurement for this known[15] compound in benzene gave MW = 798 (647 calculated for a monomer). This compound exhibits an IR spectrum similar to that of **4**.

(34) This experiment also establishes that isotopic exchange[4c,10] between the An–H functionality and the deuterated solvent is slow on the time scale of the kinetic measurements.

(35) (a) Marks, T. J. *Astract of Papers*, 197th National Meeting of the American Chemical Society, Dallas, TX, April 9–14, 1989; American Chemical Society: Washington, DC, 1989; INOR 8. (b) Nolan, S. P.; Marks, T. J. *J. Am. Chem. Soc.* **1989**, *111*, 8538–8540.

Table II. Second-Order Rate Constant Data for Olefin Insertion into the Actinide–Hydride Bonds of Various $Cp'_2An(H)(OR)$ Complexes[a]

complex	olefin	T (°C)	k (M^{-1} s^{-1})
$Cp'_2Th(D)[OCH(t\text{-}Bu)_2]$ (**2D**)	1-hexene	60.0	2.2 (2) × 10^{-5}
$Cp'_2Th(H)[OCH(t\text{-}Bu)_2]$[b] (**2H**)	ethylene	30.0	~2 × 10^{-4}
$Cp'_2Th(H)[OCH(t\text{-}Bu)_2]$ (**2H**)	1-hexene	60.0	2.9 (1) × 10^{-5}
$Cp'_2Th(H)[OCH(t\text{-}Bu)_2]$ (**2H**)	4-methoxy-styrene	60.0	2.6 (4) × 10^{-5}
$Cp'_2Th(H)[OCH(t\text{-}Bu)_2]$ (**2H**)	styrene	60.0	1.2 (1) × 10^{-5}
$Cp'_2Th(H)[OCH(t\text{-}Bu)_2]$[c] (**2H**)	cyclohexene	60.0	NR
$Cp'_2Th(D)(O\text{-}t\text{-}Bu)$ (**1D**)	cyclohexene	60.0	3.2 (1) × 10^{-4}
$Cp'_2Th(H)(O\text{-}t\text{-}Bu)$[d] (**1H**)	1-hexene	30.0	>10^{-2}
$Cp'_2Th(H)(O\text{-}t\text{-}Bu)$[d] (**1H**)	styrene	30.0	>10^{-2}
$Cp'_2Th(H)(O\text{-}t\text{-}Bu)$[e] (**1H**)	cyclohexene	60.0	2.7 (1) × 10^{-4}
$Cp'_2Th(H)(O\text{-}t\text{-}Bu)$ (**1H**)	cyclohexene	60.0	4.6 (2) × 10^{-4}
		70.0	6.6 (3) × 10^{-4}
		80.0	1.08 (4) × 10^{-3}
		90.0	1.49 (2) × 10^{-3}
$Cp'_2U(H)(O\text{-}t\text{-}Bu)$[d] (**4**)	1-hexene	30.0	>10^{-2}
$Cp'_2U(H)(O\text{-}t\text{-}Bu)$[d] (**4**)	styrene	30.0	>10^{-2}
$Cp'_2U(H)(O\text{-}t\text{-}Bu)$ (**4**)	cyclohexene	30.0	1.6 (1) × 10^{-4}

[a] All kinetic measurements were carried out in toluene-d_8 except where noted. [b] This rate is approximate because of the uncertainties in measuring concentrations of gaseous ethylene. [c] No reaction was observed over a period of 1 week. [d] Rates were too fast to be measured accurately by NMR techniques. [e] Rate measured in THF-d_8.

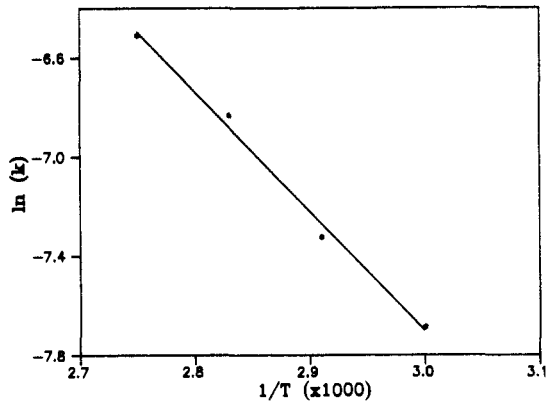

Figure 3. Arrhenius plot for the reaction of cyclohexene with $Cp'_2Th(H)(O\text{-}t\text{-}Bu)$ (**1H**). Units: k, M^{-1} s^{-1}; T, K.

could not be measured with acceptable accuracy.

In regard to activation parameters for olefin insertion, analysis of the **1H** + cyclohexene system from 60.0 to 90.0 °C (Figure 3) yields, by least-squares analysis, E_a = 9.7 (5) kcal/mol, A = 9.9 (3) × 10^2; $\Delta H^{\ddagger}$ = 9.0 (5) kcal/mol, and $\Delta S^{\ddagger}$ = −47.2 (1) eu. The effect of ethereal-coordinating solvents on this reaction was found to be small but significant, with $k_{THF}/k_{toluene}$ = 0.59 (5). Measurement of $k_{Th\text{-}H}/k_{Th\text{-}D}$ kinetic isotope effects at 60.0 °C for **1H**/**1D** + cyclohexene and **2H**/**2D** + 1-hexene yielded 1.4 (1) and 1.3 (2), respectively. In regard to metal effects, the rate constant for $Cp'_2Th(H)(O\text{-}t\text{-}Bu)$ + cyclohexene is estimated to be 1.1 × 10^{-4} M^{-1} s^{-1} at 30.0 °C from extrapolation of the Arrhenius plot (Figure 3). In comparison, the rate constant for $Cp'_2U(H)(O\text{-}t\text{-}Bu)$ + cyclohexene at 30.0 °C is found to be only slightly larger, 1.6 (1) × 10^{-4} M^{-1} s^{-1} (Table II). From Table II it can also be seen that, for constant metal and olefin, ancillary ligand effects on insertion rates can be very large. Thus, from the relative rates of **2H**/**1H** + 1-hexene and **2H**/**1H** + cyclohexene it is concluded[36] that $k_{O\text{-}t\text{-}Bu}/k_{OCH(t\text{-}Bu)_2} \gtrsim 10^3$. Concerning olefin effects on the insertion rate for constant organoactinide complex, it can be seen in Table II that for $Cp'_2Th(H)[OCH(t\text{-}Bu)_2]$, the relative rates are ethylene > 1-hexene > 4-methoxystyrene > styrene ≫ cyclohexene. It is noteworthy that the π-releasing 4-methoxy substituent accelerates the rate of styrene insertion by a factor of 2.2 (5).

Diastereoselection in the Insertion Reactions of Organoactinide Hydrides Having Chiral Alkoxide Ligands. The large, presumably steric ancillary ligand effects observed for olefin insertion (vide supra) raise the question of whether chiral alkoxide ancillary ligands might exert a stereodifferentiating influence on the course of actinide-centered olefin insertion reactions.[37] Such ligands are readily available from the natural chiral pool and can be straightforwardly incorporated into organoactinide hydrides (eqs 3–8). Experiments were carried out with chiral alkoxide ligands of varying steric demands. Substrates included *unfunctionalized* olefins (traditionally the most difficult upon which to effect transition-metal-centered enantioselective transformations[37-39]) of varying steric requirements (*cis*-2-butene, norbornene) and unfunctionalized ketones of differing steric bulk (acetophenone, butyrophenone). The stereochemical outcome of these reactions was conveniently monitored by NMR spectroscopy, in which the paramagnetic ($5f^2$) U(IV) center induces large isotropic shifts with relatively narrow line widths.[4,40] As exemplified by Figure 4, the appreciable chemical shift dispersion allows differentiation (especially from the Cp′ signals) of major diastereomers. A similar analysis of the diamagnetic **9** + norbornene system was also possible with careful field shimming at 400 MHz. In analysis of insertion processes involving norbornene, it was assumed that only organoactinide products of exo regiochemistry are formed in significant quantities (eq 13), which, to our knowledge, obtains for all other transition metal hydride additions to this olefin.[41-46]

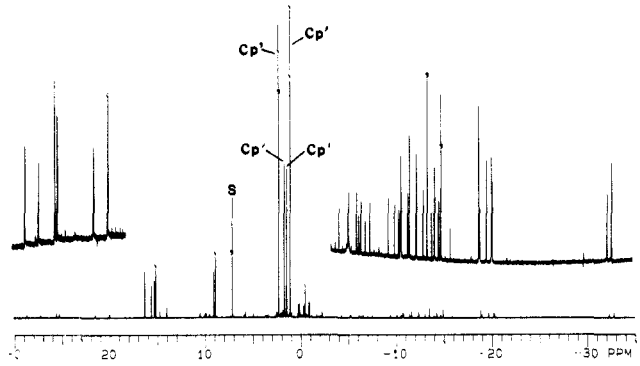

Figure 4. ^1H NMR spectrum (400 MHz) of a mixture of two diastereomeric Cp'_2U(*exo*-2-norbornyl){[(1*S*)-*endo*]-bornoxide} complexes (**11**).

(36) Assuming E_a = 10 kcal/mol for $Cp'_2Th(H)[OCH(t\text{-}Bu)_2]$ + 1-hexene, k(30 °C) ≈ 6.5 × 10^{-6} M^{-1} s^{-1}.

(37) For leading references in asymmetric homogeneous catalysis, see: (a) Brown, J. M. *Chem. Br.* **1989**, *25*, 276–280. (b) Noyori, R. *Chem. Soc. Rev.* **1989**, *18*, 187–208. (c) Brunner, H. *Synthesis* **1988**, 645. (d) Bosnich, B., Ed. *Asymmetric Catalysis*; NATO ASI Series E 103; Martinus Nijhoff Publishers: Dordrecht, Holland, 1986. (e) Morrison, J. D., Ed. *Asymmetric Synthesis*; Academic Press: Orlando, FL, 1985; Vol. 5. (f) Kagan, H. B. In *Comprehensive Organometallic Chemistry*; Wilkinson, G., Stone, F. G. A., Abel, E. W., Eds.; Pergamon Press: Oxford, 1982; Chapter 53.

(38) (a) Takaya, H.; Ohta, T.; Sayo, N.; Kumobayashi, H.; Akutagawa, S.; Inoue, S.; Kasahara, I.; Noyori, R. *J. Am. Chem. Soc.* **1987**, *109*, 1596–1597, and references therein. (b) Halpern, J. *Pure Appl. Chem.* **1983**, *55*, 99–106. (c) Knowles, W. S. *Acc. Chem. Res.* **1983**, *16*, 106–112. (d) Halpern, J. *Science (Washington, D.C.)* **1982**, *217*, 401–408. (e) Fryzuk, M.; Bosnich, B. *J. Am. Chem. Soc.* **1977**, *99*, 6262–6267.

(39) (a) Halterman, R. L.; Vollhardt, K. P. C. *Organometallics* **1988**, *7*, 883–892. (b) Halterman, R. L.; Volhardt, K. P. C.; Welker, M. E.; Bläser, D.; Boese, R. *J. Am. Chem. Soc.* **1987**, *109*, 8105–8107. (c) Paquette, L. A.; McKinney, J. A.; McLaughlin, M. L.; Rheingold, A. L. *Tetrahedron Lett.* **1986**, *27*, 5599–5602. (d) Cesarotti, E.; Ugo, R.; Vitiello, R. *J. Mol. Catal.* **1981**, *12*, 63–69. (e) Cesarotti, E.; Ugo, R.; Kagan, H. B. *Angew. Chem., Int. Ed. Engl.* **1979**, *18*, 779–780.

(40) (a) Fischer, R. D. In ref 4b, Chapter 8. (b) Fischer, R. D. In *Organometallics of the f-Elements*; Marks, T. J., Fischer, R. D., Eds.; Reidel: Dordrecht, Holland, 1978; Chapter 11.

(41) Ojima, I.; Hirai, K. In ref 37d, Chapter 4, and references therein.

(42) Hydrocyanation: (a) Hodgson, M.; Parker, D.; Taylor, R. J.; Ferguson, G. *Organometallics* **1988**, *7*, 1761–1766, and references therein. (b) Bäckvall, J. E.; Andell, O. S. *J. Chem. Soc., Chem. Commun.* **1981**, 1098–1099.

(43) (a) Hydrosilylation: Hayashi, T.; Tamao, K.; Katsuro, Y.; Nakae, I.; Kumada, M. *Tetrahedron Lett.* **1980**, *21*, 1871–1874. (b) Hydroboration: Brown, H. C.; Kawakami, J. H.; Liu, K. T. *J. Am. Chem. Soc.* **1973**, *95*, 2209–2216.

(44) Hydroalkenylation: (a) Bogdanović, B.; Henc, B.; Meister, B.; Pauling, H.; Wilke, G. *Angew. Chem., Int. Ed. Engl.* **1973**, *12*, 954–964. (b) Bogdanović, B. *Angew. Chem., Int. Ed. Engl.* **1973**, *12*, 954–964.

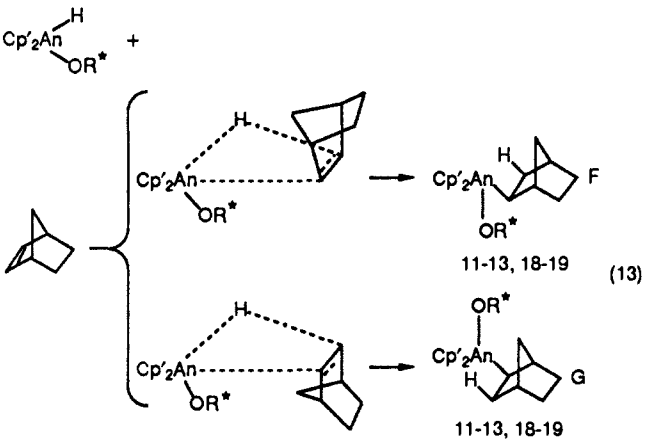

(13)

11: An = U, OR* = [(1*S*)-*endo*]-bornoxide
12: An = Th, OR* = [(1*S*)-*endo*]-bornoxide
13: An = U, OR* = (1*R*, 2*S*, 5*R*)-menthoxide
18: An = U, OR* = (*R*)-2-butoxide
19: An = U, OR* = (1*S*, 2*S*, 5*R*)-neomenthoxide

In the present study, this and NMR-derived conclusions about diastereoselectivity are supported by independent chemical evidence (vide infra).

Table III shows the results of the $Cp'_2An(H)(OR^*)$ + substrate diastereoselectivity studies. It is evident that sterically less-demanding alkoxide ancillary ligands (2-butoxide) and olefins (*cis*-2-butene) afford minimal diastereoselection. Similar results are observed with acetophenone and butyrophenone. The greatest diastereoselectivities are observed for the addition of bulky norbornene to hydrides having sterically demanding alkoxide coligands (menthoxide, bornoxide, neomenthoxide). Interestingly, the de results for these ligands are rather similar, as is the increase upon lowering the temperature (Table III). A control experiment in which the **8** + norbornene reaction was monitored to completion by NMR at −45 °C yielded within experimental error, a de indistinguishable from that obtained when the reaction was carried out in a −45 °C refrigerated bath followed by NMR analysis at room temperature. Thus, there is no evidence for significant product racemization on the time scale of the room temperature NMR analysis. To establish absolute configuration, the product of the room temperature **8** + norbornene reaction (**11**) was treated with CO_2 then aqueous HCl to yield, after workup, a mixture of norbornane-2-carboxylic acids (eq 14, see Experimental Section

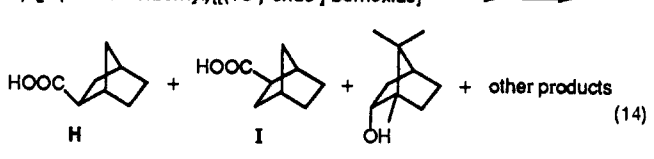

H I (14)

for details). ^1H NMR spectroscopy indicated that the regiochemistry was exclusively (≥95%) exo.[21a] Polarimetry measurements[21b] established that the major enantiomer is the (−)-carboxylic acid (**I** corresponding to precursor complex structure **G**) with 21% ee. This ee value agrees well with the ^1H NMR results (Table III).

Several experiments were also carried out to determine whether the diastereomeric actinide alkyl insertion products exhibited differential reactivities. The rates of isomerization of the two $Cp'_2U(sec\text{-butyl})[(1R,2S,5R)\text{-menthoxide}]$ products to the identical *n*-butyl product (cf., eq 10) were monitored by NMR and found to be indistinguishable. Exposure of the diastereomeric norbornyl mixtures **11** and **12** to gaseous hydrogen effected rapid hydrogenolysis,[12] regenerating the starting $Cp'_2An(H)(OR^*)$ complexes and producing norbornane. For each mixture, the rates of hydrogenolysis of the component diastereomers were indistinguishable by ^1H NMR.

Table III. Diastereomeric Excess (de) Values[a] in C_6D_6 for the Insertion Reactions of Chiral Actinide Hydride Complexes with Olefins and Ketones

complex	olefin or ketone	reactn temp (°C)	de value (%)
$Cp'_2U(H)[(1R,2S,5R)$-methoxide] (**5**)	norbornene	22	22
		0	29[b]
		−30	28[b]
$Cp'_2U(H)[(1R,2S,5R)$-menthoxide] (**5**)	*cis*-2-butene	22	5
$Cp'_2U(H)[(1R,2S,5R)$-menthoxide] (**5**)	acetophenone	22	6
$Cp'_2U(H)[(1R,2S,5R)$-menthoxide] (**5**)	butyrophenone	22	10
$Cp'_2U(H)[(R)$-2-butoxide] (**7**)	norbornene	22	0
$Cp'_2U(H)\{[(1S)$-*endo*]-bornoxide] (**8**)	norbornene	22	24
		−30	33[b]
		−45	36[b]
$Cp'_2Th(H)\{[(1S)$-*endo*]-bornoxide} (**9**)	norbornene	22	18
$Cp'_2U(H)[(1S,2S,5R)$-neomenthoxide] (**10**)	norbornene	22	25

[a] Estimated uncertainties in de values are ±2%. [b] DE values measured in toluene-d_8.

Relative Energetics of Various Olefin Approach Pathways. To better understand in a qualitative sense the stereochemistry of olefin–hydride addition in the present and ultimately in other chiral f-element systems,[13] molecular mechanics calculations were performed on several hypothetical olefin approach trajectories and the results examined with molecular graphics techniques (see Experimental Section for details). The goal was to examine gross steric factors during the initial approach of an olefin toward the $Cp'_2An(H)(OR^*)$ reaction center. While such analyses[47] are necessarily approximate in nature due, among other factors, to uncertainties in the metal–ligand force field, the present treatment benefits greatly from the limited degrees of freedom allowed by the reactants and by the questions being asked. Thus, a large body of Cp'_2AnX_2, $Cp'_2An(X)Y$, and $Cp'_2AnX_2(Y)$ structural data argues that the primary coordination sphere in these organoactinide systems is rather rigid.[4a,b,11,24] Since the present inquiry focuses upon gross interligand/intermolecular steric interactions, the sterically encumbered norbornene + $Cp'_2U(H)\{[(1S)$-*endo*]-bornoxide} system was chosen. This system exhibits the largest de values, the absolute configuration of addition is known, and an extremely bulky olefin and ancillary alkoxide are involved. The latter characteristics should accentuate nonbonded interactions. Moreover, the rigid geometries of the olefin and alkoxide reduce the degrees of freedom encountered in analyzing various approach pathways vis-à-vis more conformationally mobile reactants. In regard to the metal–ligand force field employed, reliable vibrational data are available. Moreover, we seek the *relative* energetics of various olefin approach pathways (A–C), so that it is physically reasonable to assume that inaccuracies in the force field will largely cancel. Confirmation of this assumption is provided by the observation that substantial, deliberate excursions in a number of key parameters (see Experimental Section) had only minor effects on *relative* energetics and that van der Waals interactions dominate the energetics.

Calculations were carried along three plausible olefin approach trajectories. Pathways A and B describe stereodifferentiating trajectories in the equatorial girdle between the U–H and U–O vectors while C describes approach from the "side". For each set of *d*, α, and β parameters, the energy of the structure was calculated by allowing rotation about the alkoxide C–O bond and the Cp′ ring centroid–U vectors. Negligible metal–ligand bond formation is expected at *d* values > 5 Å. Figure 5A shows the calculated energetics of the minimum energy pathways for tra-

(45) Homogeneous hydrogenation: Hussey, A. S.; Takeuchi, Y. *J. Org. Chem.* **1970**, *35*, 643–647.
(46) Hydrogen halide addition: (a) Kwart, H.; Nyce, J. L. *J. Am. Chem. Soc.* **1964**, *86*, 2601–2606. (b) Stille, J. K.; Sonnenberger, F. M.; Kinstle, T. H. *J. Am. Chem. Soc.* **1966**, *88*, 4922–4925.
(47) For other recent applications of such techniques to homogeneous catalysis, see: (a) Bogdan, P. L.; Irwin, J. J.; Bosnich, B. *Organometallics* **1989**, *8*, 1450–1453. (b) Brown, J. M.; Evans, P. L.; Lucy, A. R. *J. Chem. Soc., Perkin Trans. 2* **1987**, 1589–1596.

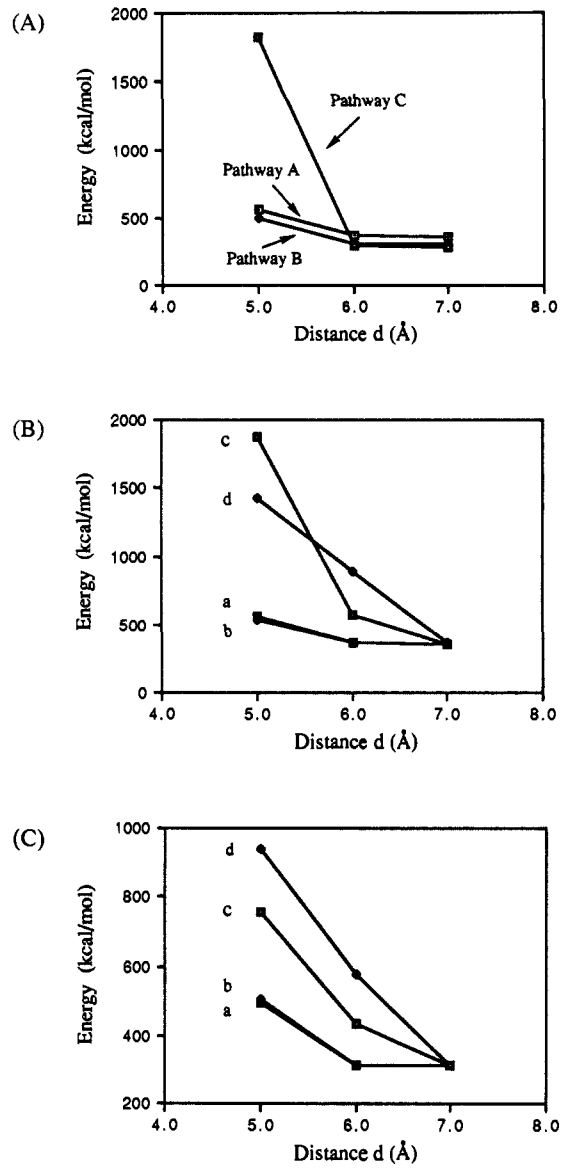

Figure 5. (A) Plot of the potential energy profile as a function of distance, d, for norbornene–$Cp'_2U(H)$[(1*S*)-*endo*]-bornoxide] approach pathways A–C with $\alpha = 50°$ and $\beta = 100°$. (B) Representative potential energy profiles as a function of distance, d, for norbornene–Cp'_2U-(H)[(1*S*)-*endo*]-bornoxide] approach pathway A: a, $\alpha = 50°$, $\beta = 100°$; b, $\alpha = 50°$, $\beta = 120°$; c, $\alpha = 60°$, $\beta = 100°$; d, $\alpha = 60°$, $\beta = 120°$. (C) Similar energy profiles as in (B) for approach pathway B.

jectories A, B, and C using the parameters indicated. In all cases, energy terms other than van der Waals make a small (<40 kcal/mol), essentially constant contribution to the total energy.[48] Most importantly, it can be seen that the steric impediments to pathway C are far larger than for A and B. Close scrutiny of the A vs B energetics (Figure 5) indicates that for all reasonable choices of α and β angles, pathway B is slightly favored for $d >$ 5 Å. At $d < 5$, situations arise where severe repulsive Cp′ methyl–norbornene bridgehead interactions raise the energy of B with respect to A. Interestingly, pathway B corresponds to the stereochemically favored course of the reaction (cf., structures **G**, **I**).

Discussion

The subject systems of this investigation differ from considerably more electron-rich systems studied previously[6,7] in that π-olefin complexes represent neither the ground state nor the detectable intermediates, and the alkyl insertion products (eq 9) are the thermodynamically favored ($\Delta H_{calc} \approx -30$ kcal/mol) end point. In regard to mechanism, free radical pathways (e.g., eqs 15 and 16)[49] appear unlikely in view of the similar insertion rates for An

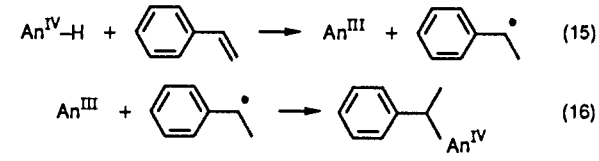

= Th and U($k_U/k_{Th} \approx 1.5$), yet greatly different An(IV) → An(III) redox properties.[4,50] Furthermore, the observed product regiochemistries and 2° → 1° isomerization rates (vide supra) seem incompatible with eqs 15 and 16.

A more reasonable scenario for olefin insertion is a four-center process (eq 17). The present kinetic data do not, a priori, dis-

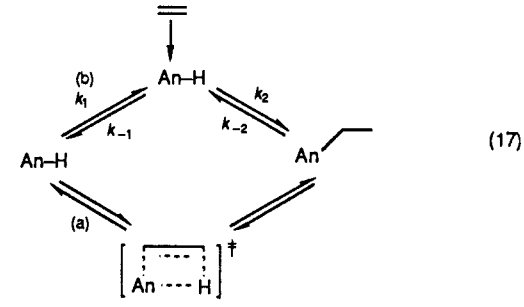

tinguish between a concerted addition pathway (a) and certain stepwise pathways (b) having a π complex intermediate. That saturation kinetics are not observed in Figure 2, that olefin complexes are not spectroscopically detected as intermediates and are unknown in An(IV) chemistry,[4] and that olefin complexation to less coordinatively saturated organolanthanides is weak and labile,[35] argues that $k_1/k_{-1} \ll 1$ and that k_{-1} is relatively large. Thermodynamic data[9c] and the observed isomerization rates argue that $k_2/k_{-2} \gg 1$. The observed Th–H/Th–D kinetic isotope effects (1.4 (1) and 1.3 (2)) are in accord with rate-limiting An–H scission and can be compared with corresponding values of 1.7 (6)–2.7 (1.0) for *intramolecular* olefin insertion in $Cp'_2Nb(C_2H_4)H$,[7a,b] 1.15 for cyclohexene insertion into $RhH_2Cl(PPh_3)_2$,[7e] and 1.58 (internal) and 1.68 (terminal) for the hydroboration of styrene.[51] Assuming negligible tunneling, a maximum theoretical Th–H/Th–D kinetic isotope effect of ca. 2.4 is estimated at 60 °C.[52]

Interestingly and in contrast to less saturated organo-f-element complexes (e.g., Cp'_2LnR[3,10]), the influence of a coordinating solvent (THF) on the rate of olefin insertion is rather small for $Cp'_2An(H)(OR)$. Considering the large steric bulk about the actinide centers in the present case, it is likely that nonbonded interactions diminish the effectiveness of THF competition for

(48) (a) The majority of the present calculations (e.g., those shown in Figure 5) employed a Lennard-Jones 12-6 intermolecular pair potential model function[48b,c] to account for van der Waals interactions. It was felt that this "harder" potential function would best differentiate among crucial nonbonded interactions operative along the various reaction pathways. A parallel series of calculations was also carried out using the "softer" MMP2 force field. While the range of calculated energies was proportionately smaller, the relative energetic ordering of the various reaction pathways was unchanged. For further discussions of the parameterization of nonbonded interactions in common molecular mechanics force fields, see refs 48d–g. (b) Berg, U.; Sandström, J. *Adv. Phys. Org. Chem.* **1989**, *25*, 1–97. (c) Maitland, G. C.; Rigby, M.; Smith, E. B.; Wakeham, W. A. *Intermolecular Forces*; Clarendon Press: Oxford, 1981; Chapters 1 and 9. (d) Lii, J.-H.; Allinger, N. L. *J. Am. Chem. Soc.* **1989**, *111*, 8576–8582, and references therein. (e) Burkert, U.; Allinger, N. L. *Molecular Mechanics*; ACS Monograph 177; American Chemical Society: Washington, DC, 1982; Chapter 2. (f) Fitzwater, S.; Bartell, L. S. *J. Am. Chem. Soc.* **1976**, *98*, 5107–5115. (g) Engler, E. M.; Androse, J. D.; Schleyer, P. V. R. *J. Am. Chem. Soc.* **1973**, *95*, 8005–8025.

(49) Sweany, R. L.; Halpern, J. *J. Am. Chem. Soc.* **1977**, *99*, 8335–8337.

(50) (a) Weigel, F. In ref 4a, Chapter 5. (b) Bratsch, S. G.; Lagowski, J. J. *J. Phys. Chem.* **1986**, *90*, 307–312, and references therein. (c) Nugent, L. J. In *MTP Int. Rev. Sci., Inorg. Chem. Series Two*, 7; Bagnall, K. W., Ed.; University Park Press: Baltimore, 1976; Chapter 6. (d) Blake, P. C.; Lappert, M. F.; Atwood, J. L.; Zhang, H. *J. Chem. Soc., Chem. Commun.* **1986**, 1148–1149.

(51) Pasto, D. J.; Kang, S. Z. *J. Am. Chem. Soc.* **1968**, *90*, 3777–3780.

(52) With the use of the approximate relationship $k_1/k_2 = e^{0.7193(\nu_1-\nu_2)/T}$. Buddenbaum, W. E.; Shiner, V. J., Jr. In *Isotope Effects on Enzyme-Catalyzed Reactions*; Cleland, W. W., O'Leary, M. H., Northrop, D. B., Eds.; University Park Press: Baltimore, 1977; Chapter 1.

vacant sites in the $Cp'_2An(OR)H$ coordination sphere. As noted above, the present study also reveals a rather small metal effect ($k_U/k_{Th} = 1.5$) on the rate of olefin insertion. This result stands in contrast to $Cp'_2An(R)(OR')$ hydrogenolysis kinetics where $k_U/k_{Th} \approx 50$ (R = CH_3; R' = $CH(t\text{-}Bu)_2$).[12]

Activation parameters for $Cp'_2Th(H)(O\text{-}t\text{-}Bu)$ + cyclohexene insertion are characterized by a rather small enthalpy of activation (9.0 (5) kcal/mol) and a large, negative (even for an intermolecular reaction) entropy of activation (−47.2 (1) eu; $\Delta G^{\ddagger} = 23$ (1) kcal/mol at 25 °C). These parameters suggest a highly ordered transition state with considerable bond-making to compensate for the bond-breaking. Interestingly, $Cp'_2An(R)(OR')$-centered hydrogenolysis processes, which proceed via a four-centered transition state (eq 18),[12] exhibit rather similar

$$Cp'_2An\text{—}R + H_2 \longrightarrow Cp'_2An\cdots R \longrightarrow Cp'_2An\text{—}H + HR \quad (18)$$

activation parameters (An = Th, R = CH_2-t-Bu, R' = t-Bu, $\Delta H^{\ddagger} = 3.7$ (2) kcal/mol, $\Delta S^{\ddagger} = -50.8$ (7) eu; An = U, R = CH_3, R' = $CH(t\text{-}Bu)_2$, $\Delta H^{\ddagger} = 9$ (2) kcal/mol, $\Delta S^{\ddagger} = -45$ (5) eu) while migratory insertion of CO at $Cp'_2Th(H)(OR)$ centers appears to proceed with lower barriers ($\Delta G^{\ddagger} = 9.2$ (4) kcal/mol at −50 °C).[53] For *intramolecular* olefin insertion in $Cp'_2Nb(olefin)H$ complexes, $\Delta H^{\ddagger} = 13$–16 kcal/mol and $\Delta S^{\ddagger} = 7$ (5) eu, while in $Cp_2Nb(styrene)H$, $\Delta H^{\ddagger} = 20.7$ (7) kcal/mol and $\Delta S^{\ddagger} = 12$ (2) eu.[7a,b] For *intramolecular* ethylene insertion in *cis*-$HRh(C_2H_4)[P(i\text{-}Pr)_3]_2$, $\Delta H^{\ddagger} = 13.0$ kcal/mol and $\Delta S^{\ddagger} = -2$ eu.[7d]

In regard to relative olefin reactivities, the present pattern, ethylene > 1-hexene > styrene ≫ cyclohexene, closely parallels hydrozirconation ($Cp_2Zr(H)Cl$ orderings[1c,d,54] and appears to reflect both steric and electronic factors. However, in contrast to the zirconium-based chemistry,[1c,d,54] alkyl isomerization processes (e.g., eqs 10 and 11) are much more sluggish at $Cp'_2Th(OR)$ centers. Among the reasons for this may be the greater endothermicity of β-hydride elimination at the thorium center.[8,9] In rigorously comparing relative rates of olefin insertion, it should be noted from eq 17 that relative observed reaction rates do not necessarily describe only relative insertion reactivities in regime b. Thus, application of the steady-state approximation indicates that the observed rate constant (eq 19) is formally a composite

$$v = k_2(k_1/k_{-1})[\text{An–H}][\text{olefin}] = k[\text{An–H}][\text{olefin}] \quad (19)$$

of insertion (k_2) and preequilibrium (k_1/k_{-1}) parameters. The importance of such a π-olefin complex as a discrete intermediate presently remains unquantified, and similar reaction coordinates having such an energetically distinct species (e.g., in LiH + ethylene[55]) or proceeding continuously from reactants to a four-center transition state (e.g., in $Cp_2LnCH_3 + H_2$[56]) have theoretical precedent. In the present study, it is found that introduction of a para methoxy substituent accelerates the rate of styrene insertion by a factor of 2.2 (5). The small derived Hammett parameter of $\rho \approx -0.4$ (based upon σ^+ values[57]) is similar in size and magnitude to those observed in group 5-[7a,b] and group 8-[7c]centered intramolecular insertion processes. Not surprisingly, these electron-rich systems exhibit opposite substituent effects for styrene binding (electron acceptors strengthen binding). With reference to the insertion process only, the present ρ value could be interpreted as indicating a modest[58] charge accumulation

Scheme II

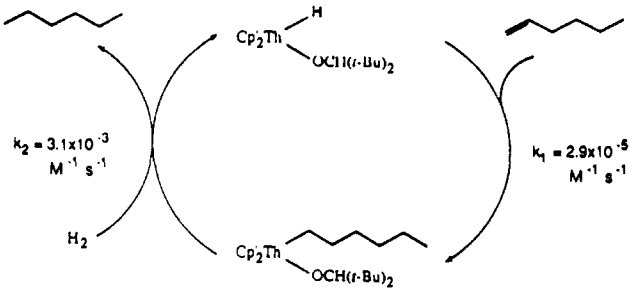

in the transition state (**J**). An identical ρ value was observed in the hydrogenolysis (eq 18) of $Cp'_2Th(p\text{-}C_6H_4X)(O\text{-}t\text{-}Bu)$ complexes.[13]

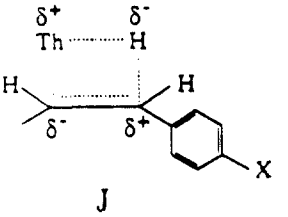

J

As noted above, the marked sensitivity of olefin insertion rates at $Cp'_2An(H)(OR)$ centers to the steric bulk of OR suggested the possibility of OR-based asymmetric induction. Studies with several chiral OR ligands, prochiral olefins, and prochiral ketones demonstrate that diastereoselectivity roughly parallels increasing steric demands of the OR groups and substrates (Table III). For norbornene, de values as high as 36% (−45 °C) are observed. To view this result in perspective, note that asymmetric transformations mediated by chiral transition-metal complexes are notoriously difficult for olefins devoid of polar substituents.[37-39] Thus, the highest reported ee values for norbornene are 40% for hydrocyanation (25 °C; many lower values have been reported),[42] 53% for hydrosilylation (25 °C),[43a] and 81% for hydroalkenylation (−97 °C; 39% at −50 °C).[44]

In regard to the relative energetics of various nonbornene approach pathways, the molecular mechanics/graphics study for An = U and OR = [(1*S*)-*endo*]-bornoxide indicates that a trajectory between the U–H and U–O bonds (ii, eq 1) is significantly favored over that from the "side" (i, eq 1). The calculations slightly favor the olefin orientation that gives rise to the observed insertion stereochemistry. This approach to Cp_2M-based asymmetric induction relies on interactions with a single chiral auxiliary in the equatorial girdle reaction plane, while the Cp' ligands play no major role in defining the asymmetry. Alternative approaches employ the entire ligation sphere to impose a rigid asymmetric environment about the reaction plane (**K**[39,59] and **L**[13]) and would appear to offer the potential for greater shape-based chiral recognition. Preliminary results[13,39,59] are in accord with this hypothesis.

K **L**

Lastly, in combination with earlier hydrogenolysis results, the present data allow a more complete description of catalytic olefin hydrogenation by a model $Cp'_2An(H)[OCH(t\text{-}Bu)_2]$ catalyst (Scheme II). The kinetic data show that the insertion and hydrogenolysis rate constants are rather closely matched and that

(53) Moloy, K. G.; Marks, T. J. *J. Am. Chem. Soc.* **1984**, *106*, 7051–7064.
(54) Hart, D. W.; Schwartz, J. *J. Am. Chem. Soc.* **1974**, *96*, 8115–8116.
(55) Hauk, K. N.; Rondan, N. G.; Schleper, P. von R.; Kaufmann, E.; Clark, T. *J. Am. Chem. Soc.* **1985**, *107*, 2821–2823.
(56) (a) Saillard, J. Y.; Hoffmann, R. *J. Am. Chem. Soc.* **1984**, *106*, 2006–2026. (b) Saillard, J. Y. Private communication.
(57) Exner, O. In *Correlation Analysis in Chemistry*; Chapman, N. B., Shorter, J., Eds.; Plenum Press: New York, 1978; Chapter 10.
(58) (a) Typical ρ values for electrophilic aromatic substitutions are in the range −6 to −13.[58b,c] (b) Carey, F. A.; Sundberg, R. J. *Advanced Organic Chemistry*, 2nd ed.; Plenum Press: New York, 1984; Part A, pp 455–520. (c) Rys, P.; Skrabal, P.; Zollinger, H. *Angew Chem., Int. Ed. Engl.* **1972**, *11*, 874–883.
(59) (a) Kaminsky, W.; Külper, K.; Brintzinger, H. H.; Wild, R. W. P. *Angew. Chem., Int. Ed. Engl.* **1985**, *24*, 507–508. (b) Kaminsky, W. *Angew. Makromol. Chem.* **1986**, *145/146*, 149–160. (c) Röll, W.; Brintzinger, H. H.; Rieger, B.; Zolk, R.; *Angew. Chem., Int. Ed. Engl.* **1990**, *29*, 279–280, and references therein.

the identity of the turnover-limiting step will depend upon the relative olefin and hydrogen concentrations. Neither of these rate constants is particularly large in comparison to other f-element catalysts. Thus, hydrogenolysis is turnover-limiting in the analogous mechanism for $(Cp'_2LuH)_2$-catalyzed hydrogenation of 1-hexene, and $k_2 \approx 7.7 \times 10^3\ M^{-1}\ s^{-1}$ ($k_1 \gtrsim 10^2$–$10^3\ M^{-1}\ s^{-1}$).[10d] Olefin addition is turnover-limiting for the corresponding hydrogenation of cyclohexene and $k_1 \approx 2.3 \times 10^{-2}\ M^{-1}\ s^{-1}$.[10d] The present results show that k_1 is sterically very sensitive, and the simple transposition of $OCH(t\text{-}Bu)_2 \rightarrow O\text{-}t\text{-}Bu$ affects a ca. 10^3 increase in k_1. Our earlier results[12] show that k_2 is sensitive to the electrophilicity at the metal center (which is depressed by OR introduction) and the Th–C bond enthalpy. As judged by variation in OR, k_2 is (not surprisingly) sterically rather insensitive. The greater hydrogenolytic reactivity of U–C bonds vis-à-vis Th–C bonds apparently reflects electronic factors that do not dominate An–H olefin insertion chemistry.

Acknowledgment. We are grateful to the NSF for support of this research under Grant CHE-8800813. We thank Dr. Michal Sabat for helpful discussions regarding the molecular mechanics calculations.

The Nature of π–π Interactions

Christopher A. Hunter and Jeremy K. M. Sanders*

Contribution from the Cambridge Centre for Molecular Recognition, University Chemical Laboratory, Lensfield Road, Cambridge CB2 1EW, United Kingdom. *Received January 30, 1990*

Abstract: A simple model of the charge distribution in a π-system is used to explain the strong geometrical requirements for interactions between aromatic molecules. The key feature of the model is that it considers the σ-framework and the π-electrons separately and demonstrates that net favorable π–π interactions are actually the result of π–σ attractions that overcome π–π repulsions. The calculations correlate with observations made on porphyrin π–π interactions both in solution and in the crystalline state. By using an idealized π-atom, some general rules for predicting the geometry of favorable π–π interactions are derived. In particular a favorable offset or slipped geometry is predicted. These rules successfully predict the geometry of intermolecular interactions in the crystal structures of aromatic molecules and rationalize a range of host–guest phenomena. The theory demonstrates that the electron donor–acceptor (EDA) concept can be misleading: it is the properties of the atoms at the points of intermolecular contact rather than the overall molecular properties which are important.

Strong attractive interactions between π-systems have been known for over half a century. They control such diverse phenomena as the vertical base–base interactions which stabilize the double helical structure of DNA,[1] the intercalation of drugs into DNA,[1,2] the packing of aromatic molecules in crystals,[3] the tertiary structures of proteins,[4] the conformational preferences and binding properties of polyaromatic macrocycles,[5] complexation in many host–guest systems,[6] and porphyrin aggregation.[7] To date, no readily accessible or intuitive model has been suggested to explain the experimental observations. Full ab initio calculations have been carried out for a limited number of small systems[8] and these do reproduce the experimental results well, but they do not explain the basic mechanisms of π–π interactions in a way that is helpful or predictive for the practical chemist. We believe that the pictorial model presented here and the rules we derive from it have a general applicability. In essence, the model indicates that the geometries of π–π interactions are controlled by electrostatic interactions but that the major energetic contribution comes from other factors.

This work was stimulated by our experimental results on porphyrin–porphyrin interactions.[5a,b] The model not only reproduces these results remarkably well, it also throws light on the whole question of π–π interactions in general. We show that π–π interactions are not due to an attractive electronic interaction between the two π-systems but occur when the attractive interactions between π-electrons and the σ-framework outweigh unfavorable contributions such as π-electron repulsion. We explain the continuum of attractive geometries that extends from the edge-on relationship that is well-known in the crystal structures of simple aromatics[3] to a coplanar, offset geometry similar to that found in porphyrins.[5c] The model implies that the donor–acceptor concept can be misleading when used to describe π–π interactions: it is the properties of the atoms in the regions of intermolecular contact that control the strength and geometry of interactions, rather than the overall molecular oxidation or reduction potentials.

Experimental Observations on Porphyrin Aggregation

Strong attractive interactions between two porphyrins lead to aggregation in solution.[7] Both in solution and crystals the two porphyrins adopt a cofacial arrangement with their centers offset.[5c,9] This geometry may be summarized as follows: (1) The π-systems of two neighboring porphyrins are parallel, with an interplanar separation of 3.4–3.6 Å. (2) The π-stacked porphyrins

(1) Saenger, W. *Principles of Nucleic Acid Structure*; Springer-Verlag: New York, 1984; pp 132–140.
(2) Wakelin, L. P. G. *Med. Res. Rev.* **1986**, *6*, 275–340.
(3) Desiraju, G. R.; Gavezzotti, A. *J. Chem. Soc., Chem. Commun.* **1989**, 621–623, and references cited therein.
(4) Burley, S. K.; Petsko, G. A. *Adv. Protein Chem.* **1988**, *39*, 125–192, and references cited therein.
(5) (a) Hunter, C. A.; Meah, N. M.; Sanders, J. K. M. *J. Am. Chem. Soc.* In press. (b) Anderson, H. L.; Hunter, C. A.; Meah, N. M.; Sanders, J. K. M. *J. Am. Chem. Soc.* In press. (d) Hunter, C. A.; Leighton, P.; Sanders, J. K. M. *J. Chem. Soc., Trans. Perkin 1* **1989**, 547–552.
(6) (a) Askew, B.; Ballester, P.; Buhr, C.; Jeong, K. S.; Jones, S.; Parris, K.; Williams, K.; Rebek, J., Jr. *J. Am. Chem. Soc.* **1989**, *111*, 1082–1090. (b) Zimmerman, S. C.; VanZyl, C. M.; Hamilton, G. S. *J. Am. Chem. Soc.* **1989**, *111*, 1373–1381. (c) Shepodd, T. J.; Petti, M. A.; Dougherty, D. A. *J. Am. Chem. Soc.* **1988**, *110*, 1983–1985. (d) Ferguson, S. B.; Diederich, F. *Angew. Chem., Int. Ed. Engl.* **1986**, *25*, 1127–1129. (e) Diederich, F. *Angew. Chem., Int. Ed. Engl.* **1988**, *27*, 362–386. (f) Jazwinski, J.; Blacker, A. J.; Lehn, J.-M.; Cesario, M.; Guilhem, J.; Pascard, C. *Tetrahedron Lett.* **1987**, *28*, 6057–6060. (g) Sheridan, R. E.; Whitlock, H. W. *J. Am. Chem. Soc.* **1988**, *110*, 4071–4073. (h) Schneider, H.-J.; Blatter, T.; Simova, S.; Theis, I. *J. Chem. Soc., Chem. Commun.* **1989**, 580–581. (i) Ortholand, J.-Y.; Slawin, A. M. Z.; Spencer, N.; Stoddart, J. F.; Williams, D. J. *Angew. Chem., Int. Ed. Engl.* **1989**, 1394–1395, and references cited therein.
(7) (a) Alexander, A. E. *J. Chem. Soc.* **1937**, 1813–1816. (b) Hughes, A. *Proc. R. Soc. London, Ser. A* **1936**, *155*, 710–711. (c) Abraham, R. J.; Eivazi, F.; Pearson, H.; Smith, K. M. *J. Chem. Soc., Chem. Commun.* **1976**, 698–699. (d) Abraham, R. J.; Eivazi, F.; Pearson, H.; Smith, K. M. *J. Chem. Soc., Chem. Commun.* **1976**, 699–701.
(8) (a) Langlet, J.; Claverie, P.; Caron, F.; Boeuve, J. C. *Int. J. Quantum Chem.* **1981**, *19*, 299–338. (b) Price, S. L.; Stone, A. J. *J. Chem. Phys.* **1987**, *86*, 2859–2868, and references cited therein.
(9) Scheidt, W. R.; Lee, Y. J. *Structure Bonding 64*; Springer-Verlag: Berlin, Heidelberg, 1987.

0002-7863/90/1512-5525$02.50/0